

# National Geospatial-Intelligence Agency



## Generation and Application of RPC Uncertainty Parameters

January 2012

(significant portions of Appendix A and Appendix B removed in accordance with general distribution)

Minor corrections/updates to the document: October 2012; typo corrected December 2012

Prepared by: John Dolloff, Hank Theiss, Scott Lee

Lead: John Dolloff ([john.t.dolloff.ctr@nga.mil](mailto:john.t.dolloff.ctr@nga.mil))

Sensor Geopositioning Center (IBR)

## Table of Contents

1.0 Introduction	4
2.0 Generation of RPC Uncertainty Parameters	8
2.1 Assumptions	8
2.2 Inputs	9
2.3 Outputs	10
2.4 Computations	10
2.4.1 Computation of image/ground plane partial derivative matrix	12
3.0 Application of RPC Uncertainty Parameters: Monoscopic Error Propagation	13
3.1 Monoscopic Absolute Error Propagation	14
3.1.1 Assumptions	14
3.1.2 Inputs	14
3.1.3 Outputs	14
3.1.4 Computations	15
3.2 Monoscopic Relative Error Propagation	16
3.2.1 Assumptions	16
3.2.2 Inputs	16
3.2.3 Outputs	17
3.2.4 Computations	17
4.0 Application of RPC Uncertainty Parameters: Stereo Error Propagation	19
4.1 Assumptions	19
4.2 Inputs	19
4.3 Outputs	20
4.4 Computations	20
5.0 References	21

Appendix A: Comparison of Results: Physical versus RPC Sensor Model	23
Appendix B: “Status of RPC Sensor Model, SGC, 14 March 2011” with Postscript	24
Appendix C: RPC00B TRE Description	28
Appendix D: Unmodeled Errors	30
Appendix E: Conversion of the Physical Sensor Model: Unrectified to Rectified	31
Appendix F: Evaluation of <i>CE</i> and <i>LE</i>	33
Appendix G: Generation of Correlation Functions	34
Appendix H: Ancillary Stereo Computations	41
Appendix I: Calculation of non-baseline x*-y* directions	45
Appendix J: Effects of x*-y* directions	48
Appendix K: Trade Studies	53

## 1.0 Introduction

This document describes both the generation and application of RPC uncertainty parameters.

The Rational Polynomial Coefficient (RPC) sensor model and corresponding image support data are widely used in the geopositioning community and are intended to replace the physical sensor model and its corresponding image support data. The RPC uncertainty parameters are included in the RPC image support data and represent its uncertainty or errors. The RPC image support data is generated “upstream” of the user community (RPC exploiters) using the physical sensor model and its corresponding image support data.

Although RPC is convenient for the down-stream user community, it is only an approximation for the physical sensor model. Also, there is a significantly better replacement sensor model available than RPC that has virtually no approximation error relative to all physical sensor model functionality. It is termed “RSM”, with detailed documentation in the Manual of Photogrammetry [1], and with an easy-to-read introduction and overview in [8]. There are also CSM-compliant RSM Generator and RSM Exploiter s/w modules now available for automatic RSM generation and exploitation [2].

However, that being said, the remainder of this document addresses RPC exclusively due to both its current wide-spread availability and related and significant issues. The issues are: (1) there are currently various and conflicting definitions of the RPC uncertainty parameters, and (2) for an assumed definition, there are cases of incorrect implementation for both their generation and application. The first issue, along with a development “history” for RPC, is discussed further in Appendix B.

### RPC Uncertainty Parameters

This document presents the Sensor Geopositioning Center (SGC) recommended definition of the RPC uncertainty parameters and computational details for both their correct generation and application. In the SGC definition, RPC uncertainty parameters consist of two image-dependent scalars,  $er$  and  $eb$ , and two image-independent scalar correlation functions,  $cort$  and  $corp$ .  $er$  and  $eb$  have units of meters and are explicitly included in the RPC image support data for each image. (They are also termed ERR\_RANDOM and ERR\_BIAS.)  $er$  is a one-sigma value that represents a random or “unmodeled” error across the image, and  $eb$  is a one-sigma value that represents a systematic or bias error across the image. Systematic errors are associated with errors in the physical sensor model’s adjustable parameter values (e.g., sensor position and attitude), and unmodeled errors all remaining “high frequency” errors. Both  $er$  and  $eb$  are expressed relative to a local horizontal tangent plane corresponding to the center of the image and a nominal elevation.

$Cort$  is a scalar temporal correlation function ( $cort(\Delta t)$ ) to be published by the image vendor and represents the temporal correlation of systematic errors between same-pass images separated

in time by  $\Delta t$  seconds. It can vary by sensor type, but is seldom changed by the vendor. Similarly, *corp* is a scalar correlation function (*corp*( $\Delta l, \Delta s$ )) to be published by the image vendor and represents the correlation of unmodeled errors between two pixel locations within the same image and separated by  $\Delta l$  lines and  $\Delta s$  samples. It can vary by sensor type, but is also seldom changed by the vendor. Correlation of errors has a significant effect on error propagation. In particular, the evaluation and correct use of *cort* has a significant effect on stereo absolute error propagation, and *corp* a significant effect on mono relative error propagation.

Note that the SGC definition of RPC uncertainty parameters requires no change to the current RPC meta-data NITF tagged record extension RPC00B described in Appendix C. The “new” RPC uncertainty “parameters”, the functions *cort* and *corp*, are vendor published, and not included in RPC00B.

Adoption of this document by the various RPC generators (commercial imagery vendors) and RPC exploiters (tool vendors) will allow for consistent and optimal use of RPC uncertainty parameters - a benefit to all in the geopositioning community. Uncertainty parameters are the basis for error propagation or accuracy predictions. In many applications, reliable accuracy predictions are as important as the extracted ground coordinates. In addition, uncertainty parameters affect the ground coordinates themselves in stereo extraction and, more generally, in multi-image extractions.

### CSM-compliant Algorithms

Both the RPC uncertainty parameter generation algorithm and RPC exploitation algorithms documented herein are generic CSM-compliant algorithms, although supporting detail allows for non-use of a CSM interface if necessary. The exploitation algorithms perform error propagation for monoscopic and stereo imagery. Corresponding details for simultaneous and optimal extraction of ground coordinates are also included.

Thus, for example, a generic CSM-compliant sensor exploitation tool (SET) is capable of rigorously exploiting any CSM-compliant plugin in a sensor agnostic way; i.e. the SET doesn't care whether the plugin is a physical sensor model or a replacement sensor model such as an RPC. Hence, the most logical approach is for the community, i.e. all SET vendors, to have a single CSM-compliant RPC plugin to use to exploit any imagery whose RPC00B TRE is populated. From the commercial satellite imagery standpoint, this eliminates the need to have a specific WV OR2A CSM plugin, which exploits RPC00B; a specific WV 1B CSM plugin, which exploits its RPC00B; a specific 1B CSM plugin for GeoEye1, which exploits its RPC00B; a specific OR2A CSM plugin for GeoEye1, which exploits its RPC00B; etc. Of course, such an approach requires that all image vendors, e.g. DigitalGlobe and GeoEye, populate the elements of the RPC00B TRE using the same approach. Our experience shows that even when an image vendor has been given the opportunity to build their own RPC Generator and RPC Exploiter, the

resulting uncertainty propagation from the RPC is inconsistent with that from the physical sensor model.

### Metric Performance

Appendix A presents a detailed comparison of extraction and error propagation based on the physical sensor model and based on its RPC counterpart for commercial satellite imagery. Both the generation and application of RPC uncertainty parameters are per this document.

In particular, extraction and error propagation results using both DigitalGlobe and GeoEye imagery are presented. Both single and stereo pair imagery are analyzed, and both the physical sensor model and the RPC sensor model generated using the physical sensor model are exercised. Differences between results based on the physical sensor model and results based on RPC are presented. Error or uncertainty ellipses are also presented graphically and compared between the two sensor models

“Bottom line” results: mono and stereo extraction and error propagation results are nearly identical using the physical sensor model and using the RPC sensor model, assuming the use of the SGC recommended definitions and algorithms. In particular, extraction results do not differ, and the largest absolute error propagation difference corresponds to 7% for stereo LE (0.9p absolute vertical error), and the largest relative error propagation difference corresponds to 15% for mono CE (0.9 p relative horizontal error). Note that these differences were compiled over all mono and stereo test cases involving 8 different images and 3 different stereo pairs. Images correspond to a mix of WorldView-1, WorldView-2, and GeoEye-1 sensors.

The above results are significantly better than those achievable using previous definitions and algorithms associated with RPC uncertainty parameters. Previous definitions/algorithms typically yield error propagation differences between the physical and RPC sensor models on the order of 100% or larger for either absolute or relative accuracy. This is discussed further in Appendix A.

The SGC-based comparison results discussed above assume a zero polynomial fit error for the RPC ground-to-image function relative to the physical sensor model’s ground-to-image function. When polynomial fit error is also included, as per the baseline algorithms, RPC error propagation (accuracy prediction) is correctly and correspondingly larger than the physical sensor model’s error propagation, in accordance with polynomial fit error statistics. For the polynomials contained in the RPC00B of the vendor supplied image meta-data, polynomial fit error ranged from 0.25 to 4 pixels per image, one-sigma. The latter value can have a significantly adverse effect on the absolute accuracy of an extracted ground point, and even more so, on the relative accuracy between two points extracted in the same image.

Figure 1 presents representative 3D (one-sigma) error ellipsoids based on error propagation and corresponding to the stereo extraction of a ground point using a pair of same-pass images from

one of the above commercial satellite sensors. Both the RPC error ellipsoid and physical sensor model error ellipsoid are presented together for comparison, with the RPC error ellipsoid generated assuming no polynomial fit error. Note that the two error ellipsoids are nearly identical using the SGC recommended definitions and algorithms.

Absolute, Ground, Unresected, Control Point Error Ellipsoid Comparison

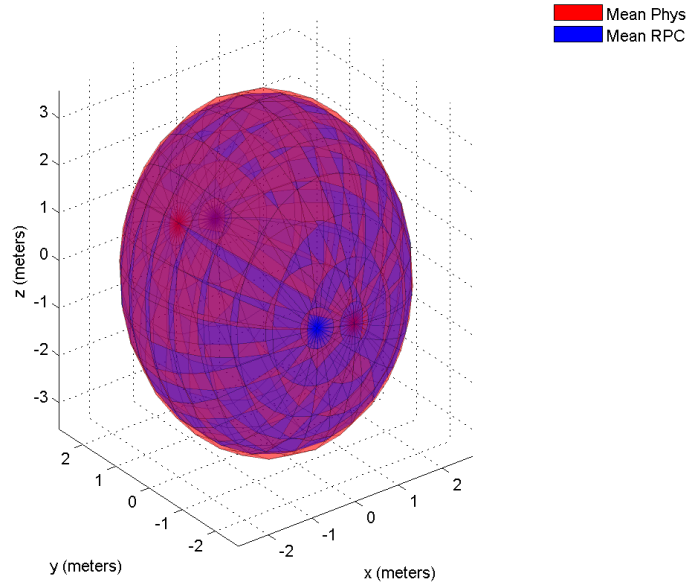


*Figure 1: RPC vs Physical Average 3D (One-Sigma) Error Ellipsoid (No Poly Fit Error)*

However, when RPC polynomial fit error is included, the RPC ellipsoid is inflated accordingly and correctly as illustrated in Figure 2. Polynomial fit error statistics were approximately 4 pixels, one sigma, across the image and computed based on a grid of check points.

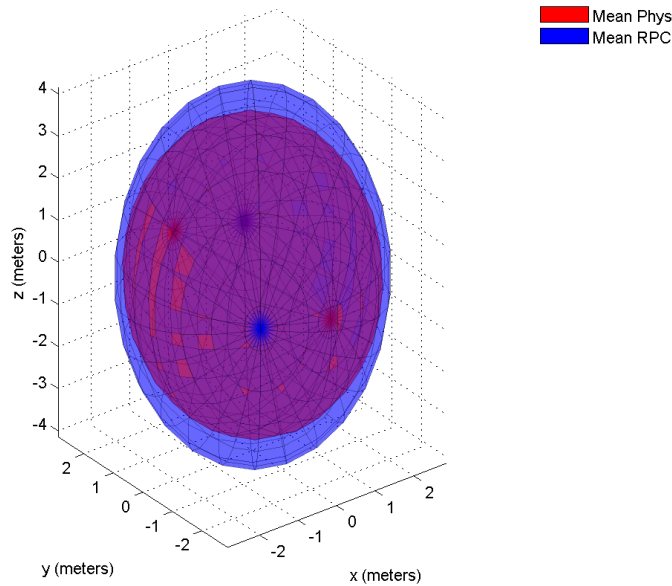


Figure 2: RPC vs Physical Average 3D (One-Sigma) Error Ellipsoid (With Poly Fit Error)

### Roadmap

Sections 2-4 go on to describe the various RPC uncertainty parameter generation and application algorithms in detail. Section 5 presents references. Numerous appendices then follow which provide various background information and further details when warranted. As mentioned earlier, Appendix A presents detailed performance results, and Appendix B a “development history” of RPC. Another major appendix is Appendix K. It presents trade studies under taken by the SGC in order to select the appropriate RPC uncertainty parameter definitions and algorithms. The major trade study involved the selection of the ground plane used to represent RPC uncertainty, i.e., the ground plane referenced by *er* and *eb*. The local horizontal tangent plane was selected. The other candidate was a ground plane perpendicular to the imaging line-of-sight vector.

## 2.0 Generation of RPC Uncertainty Parameters

The following describes the generation of RPC uncertainty parameters: *er*, *eb*, *cort*, and *corp*. Their generation assumes access to the physical sensor model via the CSM API for the image.

### 2.1 Assumptions

$Er$ ,  $eb$ ,  $cort$ , and  $corp$  are to be computed on a per image basis, i.e., a stereo pair of images is neither required nor used for their generation. ( $Cort$  and  $corp$  are actually vendor pre-computed, image-independent, correlation functions as discussed below.)

In the following, subscript “S” corresponds to sensor support data adjustable parameters/errors, subscript “U” to sensor unmodeled errors, and subscript “TU” to total unmodeled errors. The latter includes the effects of RPC polynomial fit error. Appendix D discusses the various sources of unmodeled error and their characteristics.

The temporal correlation of sensor support data errors between the current image and other “same-pass” images is accounted for via the function  $cort$ . The correlation of total unmodeled errors between two locations within the same image is accounted for via the function  $corp$ .

The physical sensor model corresponds to the appropriate image for which RPC uncertainty parameters are to be generated. That is, if the image is unrectified, the physical sensor model corresponds to the unrectified image. If the image is rectified (also known as “Ortho-Ready” in the commercial optical satellite imaging community), the physical sensor model corresponds to the rectified image. See Appendix E for a summary of conversion between these two physical sensor models.

## 2.2 Inputs

The following are inputs to the RPC uncertainty generation algorithm corresponding to a grid of points ( $i=1,\dots,25$ ) spread evenly across the entire image in a 5x5 grid (such that the edges of the grid align with the edges of the image):

$(l, s, z)_i$ , the image line and sample location and corresponding nominal elevation at grid point  $i$ , with units of pixels, pixels, and meters, respectively.

$P_{Ui}$ , the  $2 \times 2$  unmodeled error covariance for the physical sensor model relative to line and sample coordinates at grid point  $i$ , with units of pixels-squared for all components;

$P_S$ , the  $n \times n$  support data error covariance for the physical sensor model corresponding to  $n$  (active) image support data adjustable parameters (units are adjustable parameter specific);

$B_{Si}$ , the  $2 \times n$  matrix of partial derivatives of line, sample with respect to the physical sensor model’s  $n$  adjustable parameters, evaluated at the nominal ground point location  $i2g(l_i, s_i, z_i)$ , where  $i2g$  is the CSM API image-to-ground function (and  $g2i$  the ground-to-image function). The units of the components of  $B_{Si}$  are pixels/(unit of the particular adjustable parameter).

$B_{Xi}$ , the  $2 \times 3$  matrix of partial derivatives of line, sample with respect to  $X$  in units of pixels/meter evaluated at the grid point  $i$  location  $X_i$  equal to  $i2g(l_i, s_i, z_i)$ . The ground point location is represented in the primary coordinate system (WGS 84 ECF).

$P_F$ , the  $2 \times 2$  error covariance corresponding to RPC polynomial fit error relative to line and sample coordinates corresponding to an arbitrary location across the image, with units of pixels-squared, and assumed generated by an RPC polynomial fit function using a dense set of check points across the image (not fit points) that also span the volume between minimum and maximum heights in the ground space.

### 2.3 Outputs

The following are outputs from the RPC uncertainty parameters generation algorithm:

$er$  in meters,  $eb$  in meters, and the functions  $cort(\Delta t)$  (unit-less) and  $corp(\Delta l, \Delta s)$  (unit-less).

### 2.4 Computations

$$\sigma_{Si}^2 = (CE\{A_i^{-1}B_{Si}P_S B_{Si}^T A_i^{-T}\}/2.15)^2 \quad (1)$$

$$\sigma_{Ui}^2 = (CE\{A_i^{-1}P_{Ui}A_i^{-T}\}/2.15)^2 \quad (2)$$

$$\sigma_{Fi}^2 = (CE\{A_i^{-1}P_F A_i^{-T}\}/2.15)^2 \quad (3)$$

In the above equations,  $CE\{\}$  corresponds to the scalar 0.9 p circular error computed using an argument consisting of a  $2 \times 2$  covariance matrix. See Appendix F for a detailed description of the  $CE\{\}$  function. Also, the superscript “ $-T$ ” indicates the transpose of the matrix inverse.

(When  $CE\{\}$  is divided by 2.15 and then squared, it can be a more accurate estimate of the appropriate error variance than the simpler estimate  $Trace\{\}/2$ , where  $Trace\{\}$  is the trace of the  $2 \times 2$  covariance matrix, i.e., the sum of its two diagonal elements. This occurs when the error ellipsoid corresponding to the  $2 \times 2$  covariance matrix is significantly non-circular, i.e., the semi-minor axis significantly smaller than the semi-major axis.)

The computations corresponding to Equations (1-3) are performed for each grid point  $i$ .  $A_i^{-1}$  is the inverse of  $A_i$  whose computation is detailed in Section 2.4.1.  $A_i^{-1}$  is the  $2 \times 2$  matrix of partial derivatives of ground plane coordinates with respect to image coordinates at grid point  $i$ , where the ground plane is the local horizontal tangent plane.  $A_i$  and  $A_i^{-1}$  have units of pixels/meter and meters/pixel, respectively, for all components.

Note that in Equation (1), the matrix  $B_{Si}$  is used to map physical sensor model adjustable parameter uncertainty to image space, and the matrix  $A_i^{-1}$  is then used to map the image space uncertainty to uncertainty in ground plane coordinates at grid point  $i$ . The resultant  $\sigma_{Si}^2$  is the variance used to represent uncertainty or errors in both directions (axes) of the local horizontal plane. Corresponding errors in these two directions are modeled as uncorrelated, i.e., the corresponding error ellipse is circular.

Some of the inputs used in Equations (1-3) are directly available via the CSM API for the physical sensor model:  $P_S$  via `getCurrentParameterCovariance`,  $P_{Ui}$  via `getUnmodeledError`, and  $B_{Si}$  via `computeSensorPartials`, for grid points  $i = 1, \dots, 25$ .

The following computations average the above results over all  $m = 25$  grid points and then compute the RPC uncertainty parameters  $er$  and  $eb$ :

$$\sigma_S^2 = \frac{1}{m} \sum_{i=1}^m \sigma_{Si}^2 \quad (4)$$

$$\sigma_U^2 = \frac{1}{m} \sum_{i=1}^m \sigma_{Ui}^2 \quad (5)$$

$$\sigma_F^2 = \frac{1}{m} \sum_{i=1}^m \sigma_{Fi}^2 \quad (6)$$

$$\sigma_{TU}^2 = \sigma_U^2 + \sigma_F^2 \quad (7)$$

$$eb = (\sigma_S^2)^{1/2} \quad (8)$$

$$er = (\sigma_{TU}^2)^{1/2} \quad (9)$$

In addition, there are two image-independent, vendor pre-computed, scalar correlation functions:

$$cort(\Delta t) \text{ is the temporal correlation function between two same-pass images;} \quad (10)$$

$$corp(\Delta l, \Delta s) \text{ is the pixel location correlation function between two different pixel locations in the same image.} \quad (11)$$

Given a specific value  $\Delta t$  for the time between two same-pass images in seconds, the evaluation of  $cort(\Delta t)$  yields the correlation (coefficient) of RPC errors between the two images. The corresponding RPC errors exclude total unmodeled errors.

The function  $cort(\Delta t)$  is a ‘‘CSM four parameter correlation function’’ and is defined by four scalar parameters. These four parameters are published by the commercial image vendor for a particular sensor and are image independent. The specific definition of the four parameters and their pre-computation are detailed in Appendix G. If the four parameters are unavailable from the vendor, a default set of values is also presented in Appendix G.. Note that this default set of values should be specifiable data base parameters.

Given specific values  $\Delta l$  and  $\Delta s$  corresponding to the difference in line and sample pixel coordinates, respectively, for two locations in the same image, the evaluation of  $corp(\Delta l, \Delta s)$  yields the correlation (coefficient) of RPC total unmodeled errors between the two locations.

The function  $corp(\Delta l, \Delta s)$  is represented as the product of two ‘‘CSM four parameter correlation functions’’, i.e.,  $corp(\Delta l, \Delta s) = corpl(\Delta l) \cdot corps(\Delta s)$ . The two corresponding sets of four parameters are published by the commercial image vendor for a particular sensor and are image

independent. Pre-computation of these parameters (the functions  $corpl(\Delta l)$  and  $corps(\Delta s)$ ) by the vendor and its specific form are discussed further in Appendix G. If the two sets of four parameters are unavailable from the vendor, a default set of values is also presented in Appendix G. Note that these default values should be specifiable data base parameters.

In summary,  $er$  and  $eb$  are computed via Equations 8-9 above and are to be placed in RPC00B on a per image basis. The correlation functions  $cort(\Delta t)$  and  $corp(\Delta l, \Delta s)$  are to be published by the vendor in accordance with their general definitions above and their detailed definitions in Appendix G. Since RPC00B does not have metadata fields associated with these two correlations functions, their parameter values are placed into a data base that can be read by the generic CSM compliant RPC during instantiation by the SET.

#### 2.4.1 Computation of image/ground plane partial derivative matrix

The following matrix is defined as the  $2 \times 2$  partial derivative matrix of image coordinates with respect to ground plane coordinates  $x^*-y^*$  for grid point  $i$ . The ground plane is the local horizontal tangent plane at grid point  $i$ , with the  $x^*$  direction corresponding to local south and the  $y^*$  direction corresponding to local east (see Appendix K for a discussion of why this ground plane was selected as opposed to one perpendicular to the line-of-sight vector):

$$A_i \triangleq \frac{\partial(l_i, s_i)}{\partial(x_i^*, y_i^*)} \tag{12}$$

The  $x^*-y^*$  plane corresponding to an arbitrary grid point is illustrated in Figure 3:

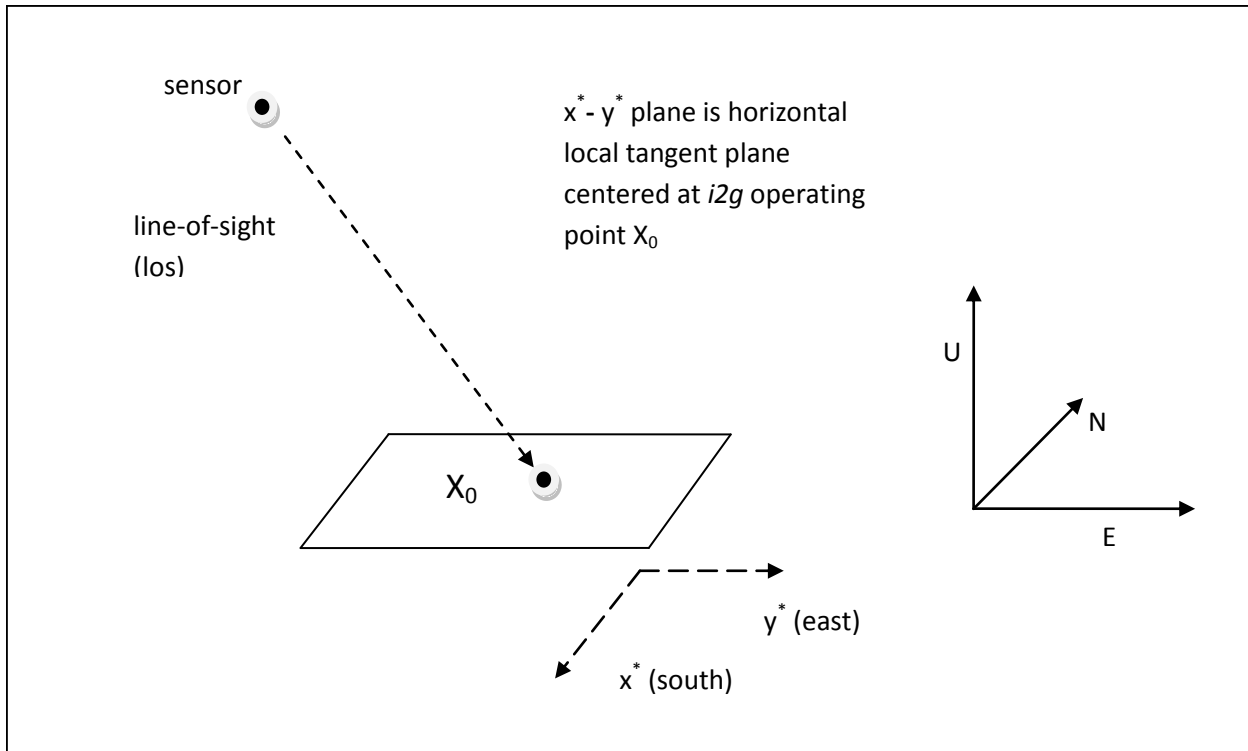


Figure 3: RPC Uncertainty is represented in the local horizontal tangent plane

The primary  $x$ - $y$ - $z$  ground coordinate system is assumed WGS-84 ECF, the coordinate system of the  $i2g$  output and  $g2i$  input via the CSM API. (When  $z_i$  is used as an input to an image-to-ground call, it is assumed (converted to) an elevation.)

Define  $\Phi_{PtoL}$  as the  $3 \times 3$  primary-to-local tangent plane coordinate system (orthonormal) transformation matrix. It is applicable at the ground (grid) point's nominal location  $X_{0i} = i2g(l_i, s_i, z_i)$  as represented in the primary coordinate system (WGS 84 ECF). The local tangent plane coordinate system is assumed ENU (east-north-up).

$B_{Xi}$  is the  $2 \times 3$  matrix of partial derivatives of  $(l, s)$  with respect to  $X$  in units of pixels/meter evaluated at the location  $X_{0i}$ . And based on the chain rule for partial derivatives:

$$A_i = \begin{bmatrix} \frac{\partial l_i}{\partial x_i^*} & \frac{\partial l_i}{\partial y_i^*} \\ \frac{\partial s_i}{\partial x_i^*} & \frac{\partial s_i}{\partial y_i^*} \end{bmatrix} = \text{left } 2 \times 2 \text{ submatrix of the } 2 \times 3 \text{ matrix } \{(B_{Xi})(\Phi_{PtoL}^T) \begin{pmatrix} 0 & 1 & 0 \\ -1 & 0 & 0 \\ 0 & 0 & 1 \end{pmatrix}\}. \quad (13)$$

### 3.0 Application of RPC Uncertainty Parameters: Monoscopic Error Propagation

This section details RPC error propagation for monoscopic extraction using  $er$ ,  $eb$ , and  $corp$ . Section 3.1 details absolute error propagation and Section 3.2 relative error propagation. All algorithms are sensor agnostic.

If a CSM plugin is not available for RPC, relevant inputs must be obtained directly from the NITF and direct RPC sensor model functionality must be available.

### 3.1 Monoscopic Absolute Error Propagation

This section details absolute error propagation corresponding to one ground point.

Note the corresponding optimal extracted ground coordinate is simply the output of the RPC image-to-ground function, or  $i2g$  (imageToGround) if the CSM interface is available.

#### 3.1.1 Assumptions

Error propagation corresponds to the use of a baseline RPC adjustment model which consists of image line offset and image sample offset adjustments. See Appendix K for a discussion on why these RPC adjustable parameters were selected.

Vendors computing the RPC uncertainty parameters  $er$  and  $eb$  as described in Section 2 should also perform monoscopic absolute error propagation at arbitrary locations within the image using both the RPC and the physical sensor models. Results are then compared for Quality Assurance, either “off-line” in a laboratory setting or “on-line” before dissemination of the RPC uncertainty parameters. Error propagation results using the two sensor models should be reasonably close.

#### 3.1.2 Inputs

The following are inputs to the RPC monoscopic absolute error propagation algorithm:

$er$  and  $eb$ , for the image, with units of meters, respectively;

$i_1 = (l_1, s_1)$ , the image coordinates in pixels corresponding to the ground point  $X_1$  of interest;

$z_1$  and  $\sigma_{0z1}$ , the ground point’s *a priori* elevation in meters and its one-sigma uncertainty in meters, respectively (if an appropriate *a priori* elevation is not available, such as from a DEM, a reference point via the CSM API (getReferencePoint), or the height offset value of the RPC can be used);

$\Sigma_1$ , the 2x2 image space mensuration error covariance corresponding to  $i_1$  in units of pixels-squared;

$i_c = (l_c, s_c, z_c)$ , the image coordinates in pixels and *a priori* elevation in meters corresponding to the center of the image.

#### 3.1.3 Outputs

The following are outputs from the RPC monoscopic absolute error propagation function:

$CovX$ , the  $3 \times 3$  ground point solution error covariance matrix in units of meters-squared and converted to a local tangent plane coordinate system;

$CE$  and  $LE$ , the corresponding 90% (or 0.9 p) horizontal and vertical accuracy predictions, respectively, in meters.

### 3.1.4 Computations

$$CovX = E\{\varepsilon X_1 \varepsilon X_1^T\} = \left( \Phi_{LtoP1} \begin{bmatrix} 0 & 0 & 0 \\ 0 & 0 & 0 \\ 0 & 0 & \sigma_{z0}^{-2} \end{bmatrix} \Phi_{LtoP1}^T + B_{X1}^T (B_{R1} P_{0R} B_{R1}^T + P_{TU1} + \Sigma_1)^{-1} B_{X1} \right)^{-1}. \quad (14)$$

In the above,  $E$  corresponds to expected value,  $\varepsilon X_1$  to the 3D error in the ground location  $X_1$ , and  $E\{\varepsilon X_1\} = 0$ , i.e., statistically the error is assumed unbiased. (Note that, throughout this document, if a vector or matrix is set equal to 0, it is understood that all corresponding components are set equal to zero.)

The following are supporting definitions/computations:

$B_{X1}$  is the  $2 \times 3$  matrix of partial derivatives of  $(l, s)$  with respect to  $X$  in units of pixels/meter evaluated at the location  $X_1$  equal to  $i2g(l_1, s_1, z_1)$ . The ground point location is represented in the primary coordinate system (WGS 84 ECF). (15)

$B_{R1}$  is the  $2 \times 2$  matrix of partial derivatives of  $(l, s)$  with respect to the baseline RPC adjustable parameters. Because these RPC adjustable parameters are line offset and sample offset, the units of  $B_{R1}$  are pixels/pixels or unit-less, and  $B_{R1} = I_{2 \times 2}$ , the  $2 \times 2$  identity matrix. (16)

$P_{0R}$  is the  $2 \times 2$  *a priori* error covariance matrix of the RPC adjustable parameters in units of pixels-squared.  $P_{0R} = eb^2 AA^T$ . (17)

The matrix  $A$  has units of pixels/meter and is computed as detailed in Section 2.4.1, with the exception that all  $i2g$  and  $g2i$  calls are via the RPC sensor model instead of the physical sensor model, and that image coordinates  $i_c$  and *a priori* elevation  $z_c$ , which correspond to the center of the image, are used instead of  $i_i$  and  $z_i$  corresponding to grid point  $i$ . (18)

Note that in Equation (17), the matrix  $A$  is used to map modeled RPC uncertainty in horizontal ground plane coordinates corresponding to the center of the image to RPC (image space) adjustable parameter uncertainty. In particular,  $P_{0R} = A \begin{bmatrix} eb^2 & 0 \\ 0 & eb^2 \end{bmatrix} A^T = eb^2 AA^T$ .

$P_{TU1}$  is the  $2 \times 2$  error covariance matrix of total RPC unmodeled error mapped to image space in units of pixels-squared.  $P_{TU1} = er^2 AA^T$ . (19)

The matrix  $\Phi_{LtoP1}$  is the local tangent plane to primary coordinate system (orthonormal) transformation matrix. It is applicable at the ground point location  $X_1$ . Note that  $\Phi_{LtoP1} = \Phi_{PtoL1}^{-1} = \Phi_{PtoL1}^T$ , where  $\Phi_{PtoL1}$  is the primary to local tangent plane transformation. (20)

If a CSM plugin is available for RPC, the above  $CovX$  is directly available via `imageToGround` (with error propagation) and in accordance with Equation (14). In addition, if needed,  $P_{0R}$  is directly available via `getCurrentParameterCovariance`,  $P_{TU1}$  via `getUnmodeledError`,  $B_{X1}$  via `computeGroundPartials`, and  $B_{R1}$  via `computeSensorPartials`.

Following the computation/receipt of  $CovX$  (Equation 14), the following final computations are performed:

Convert  $CovX$  to a local tangent plane coordinate system representation:  $\rightarrow \Phi_{PtoL1} CovX \Phi_{PtoL1}^T$ . (21)

Compute  $CE$  and  $LE$  using , i.e.,  $CE = CE\{CovX\}$ ,  $LE = LE\{CovX\}$ . (22)

### 3.2 Monoscopic Relative Error Propagation

This section details relative error propagation corresponding to two ground points measured in the same image.

Note that the corresponding optimal extracted ground coordinate for both points is simply their respective output of the CSM image-to-ground function, or `i2g` (`imageToGround`), if the CSM interface is available for the RPC model.

#### 3.2.1 Assumptions

Error propagation corresponds to the baseline RPC adjustment model which consists of image offset adjustments.

Vendors computing the RPC uncertainty parameters *er*, *eb*, and *corp* as described in Section 2 should also perform monoscopic relative error propagation at arbitrary point-pair locations within the image using both the RPC and the physical sensor models. Results are then compared for Quality Assurance before dissemination of the RPC uncertainty parameters.

#### 3.2.2 Inputs

The following are inputs to the RPC monoscopic relative error propagation algorithm:

*er* and *eb* for the image, with units of meters;

$corp(\Delta l, \Delta s)$ , the vendor published, image-independent, pixel location correlation function (unitless) with default values for its defining parameters specified in Appendix G if the published function is unavailable;

$i_i = (l_i, s_i)$ , the image coordinates in pixels corresponding to ground points  $X_i$  of interest, subscript  $i = 1, 2$ ;

$z_i$  and  $\sigma_{z_i}$ , the *a priori* elevation in meters and its one-sigma uncertainty in meters, respectively, for ground points  $X_i$ ,  $i = 1, 2$ . Because relative error propagation is to be performed,  $\sigma_{z_i}$  should statistically reflect random elevation errors only, i.e., not include any bias error between the two locations;

$\Sigma_i$ , the  $2 \times 2$  image space mensuration error covariance in units of pixels-squared for ground point image measurements  $i_i = (l_i, s_i)$ , subscript  $i = 1, 2$ ;

$i_c = (l_c, s_c, z_c)$ , the image coordinates in pixels and *a priori* elevation in meters corresponding to the center of the image;

### 3.2.3 Outputs

The following are outputs from the RPC monoscopic relative error propagation algorithm:

$CovX = E\left\{\begin{bmatrix} \varepsilon X_1 \varepsilon X_1^T & \varepsilon X_1 \varepsilon X_2^T \\ \varepsilon X_2 \varepsilon X_1^T & \varepsilon X_2 \varepsilon X_2^T \end{bmatrix}\right\}$ , the  $6 \times 6$  (two) ground point solution error covariance matrix in units of meters-squared and converted to local tangent plane coordinate system(s);

$CErel$  and  $LErel$ , the corresponding 90% horizontal and vertical relative accuracy predictions, respectively, in meters.

### 3.2.4 Computations

$$CovX = \left( \begin{bmatrix} CZinv_1 & 0 \\ 0 & CZinv_2 \end{bmatrix} + \begin{bmatrix} B_{X1}^T & 0 \\ 0 & B_{X2}^T \end{bmatrix} \left( \begin{bmatrix} B_{R1} \\ B_{R2} \end{bmatrix} [P_{OR}] [B_{R1}^T \quad B_{R2}^T] + \begin{bmatrix} P_{TU1} & P_{TU12} \\ P_{TU12}^T & P_{TU2} \end{bmatrix} + \begin{bmatrix} \Sigma_1 & 0 \\ 0 & \Sigma_2 \end{bmatrix} \right)^{-1} \begin{bmatrix} B_{X1} & 0 \\ 0 & B_{X2} \end{bmatrix} \right)^{-1} \quad (23)$$

The following are supporting definitions/computations:

$B_{X_i}$  is the  $2 \times 3$  matrix of partial derivatives of  $(l, s)$  with respect to  $X_i$ ,  $i = 1, 2$ , in units of pixels/meter and evaluated at the location  $i2g(l_i, s_i, z_i)$ . The ground point location  $X_i$  is represented in the primary coordinate system (WGS 84 ECF). (24)

$B_{Ri}$  is the  $2 \times 2$  matrix of partial derivatives of  $(l, s)$  with respect to the baseline RPC adjustable parameters. The units of  $B_{Ri}$  are pixels/pixels or unit-less.  $B_{Ri} = I_{2 \times 2}$ , independent of location  $X_i$ , and where  $I_{2 \times 2}$  is the  $2 \times 2$  identity matrix. (25)

$P_{0R}$  is the  $2 \times 2$  *a priori* error covariance matrix for the RPC adjustable parameters in units of pixels-squared.  $P_{0R} = eb^2AA^T$ . (26)

The matrix  $A$  has units of pixels/meter and is computed as detailed in Section 2.4.1, with the exception that all  $i2g$  and  $g2i$  calls are via the RPC sensor model instead of the physical sensor model, and that image coordinates  $i_c$  and *a priori* elevation  $z_c$ , which correspond to the center of the image, are used instead of  $i_i$  and  $z_i$  for grid point  $i$ . (27)

$P_{TUi}$  is the  $2 \times 2$  error covariance matrix of total RPC unmodeled errors mapped to image space in units of pixels-squared.  $P_{TUi} = er^2AA^T$ , independent of location  $X_i$ ,  $i = 1, 2$ . (28)

$P_{TU12}$  is the  $2 \times 2$  error cross-covariance matrix of total RPC unmodeled errors mapped to image space in units of pixels-squared between the two locations.  $P_{TU12} = \text{corp}(\Delta l, \Delta s) \cdot P_{TU1}$ , where  $\Delta l = |l_1 - l_2|$  and  $\Delta s = |s_1 - s_2|$ . (29)

$CZinv_i = \Phi_{LtoPi} \begin{bmatrix} 0 & 0 & 0 \\ 0 & 0 & 0 \\ 0 & 0 & \sigma_{zi}^{-2} \end{bmatrix} \Phi_{LtoPi}^T$ ,  $i = 1, 2$ , where  $\Phi_{LtoPi}$  corresponds to the ground location

$X_i$  equal to  $i2g(l_i, s_i, z_i)$ .  $CZinv_i$  represents the *a priori* information for the elevation of ground point  $i$  converted to the primary coordinate system. (30)

The matrix  $\Phi_{LtoPi}$  is the local tangent plane to primary coordinate system (orthonormal) transformation matrix applicable at location  $X_i$ . Note that  $\Phi_{LtoPi} = \Phi_{PtoLi}^T$ , where  $\Phi_{PtoLi}$  is the primary-to-local tangent plane transformation. (31)

If a CSM plugin is available for RPC, the above  $P_{0R}$  is directly available via `getCurrentParameterCovariance`,  $P_{TUi}$  via `getUnmodeledError`,  $P_{TU12}$  via `getUnmodeledCrossCovariance`,  $B_{Xi}$  via `computeGroundPartials`, and  $B_{Ri}$  via `computeSensorPartials`,  $i = 1, 2$ .

Following the computation of  $CovX$  (Equation 23), the following final computations are performed:

Convert  $CovX$  to a local tangent plane coordinate system representation:

$CovX = \begin{pmatrix} \Phi_{PtoL} & 0 \\ 0 & \Phi_{PtoL} \end{pmatrix} CovX \begin{pmatrix} \Phi_{PtoL}^T & 0 \\ 0 & \Phi_{PtoL}^T \end{pmatrix}$ , where  $\Phi_{LtoP}$  is the local tangent plane to primary coordinate system (orthonormal) transformation matrix applicable at location  $(X_1 + X_2)/2$ . (32)

Compute  $CE_{rel}$  and  $LE_{rel}$  using  $CovX$ . (33)

Note: if we express the  $6 \times 6$   $CovX$  with  $3 \times 3$  blocks,  $CovX = \begin{bmatrix} CovX_{11} & CovX_{12} \\ CovX_{21} & CovX_{22} \end{bmatrix}$ ,  $CE_{rel}$  and  $LE_{rel}$  equal  $CE$  and  $LE$  computed using the  $3 \times 3$  relative covariance matrix  $CovX_{rel} = (CovX_{11} + CovX_{22} - CovX_{12} - CovX_{21})$ , i.e.,

$$CE_{rel} = CE\{CovX_{rel}\}, \quad LE_{rel} = LE\{CovX_{rel}\}. \quad (34)$$

#### 4.0 Application of RPC Uncertainty Parameters: Stereo Error Propagation

This section details RPC (absolute) error propagation for stereo extraction using  $er$ ,  $eb$ , and  $cort$  from two same-pass stereo images. All algorithms are sensor agnostic.

Note that the error propagation algorithm is an inherent part of an optimal Weighted Least Squares (WLS) stereo extraction algorithm. See Appendix H for the entire WLS solution algorithm that includes computation of a best estimate of ground point location.

##### 4.1 Assumptions

Error propagation corresponds to the baseline RPC adjustment model which consists of image offset adjustments per image. See Appendix H for generalization to an RPC adjustment model that also includes rate terms.

Vendors computing the RPC uncertainty parameters  $er$ ,  $eb$ , and  $cort$  as described in Section 2 should also perform absolute stereo error propagation at arbitrary locations within the images using both the RPC and the physical sensor models. Results are then compared for Quality Assurance.

The following algorithm assumes two same-pass images. If they are not correlated (same-pass images), simply set the value of the correlation coefficient  $\rho = 0$  in the following algorithm.

##### 4.2 Inputs

The following are inputs to the stereo error propagation algorithm:

$er_j, eb_j$ , with units of meters for the two images  $j = 1, 2$

$cort(\Delta t)$  is the vendor-published, image-independent, temporal correlation function (unit-less) with default values for its defining parameters specified in Appendix G if the published function is unavailable;  $i_j = (l_j, s_j)$ , the image coordinates in pixels corresponding to the ground point  $X$  of interest for the two images, subscript  $j = 1, 2$ ;

$z_0$ , an *a priori* elevation in meters for the corresponding ground point;

$\Sigma_j$  , the  $2 \times 2$  image space mensuration error covariance in units of pixels-squared for image = 1,2 ;

$i_{cj} = (l_{cj}, s_{cj}, z_{cj})$  , the image coordinates in pixels and *a priori* elevation in meters corresponding to the center of image  $j$ ;

### 4.3 Outputs

The following are outputs from the stereo error propagation algorithm:

$CovX$  , the  $3 \times 3$  ground point solution error covariance matrix in units of meters-squared and converted to a local tangent plane coordinate system;

$CE$  and  $LE$  , the corresponding 90% (0.9p) horizontal and vertical accuracy predictions, respectively, in meters.

### 4.4 Computations

$CovX =$

$$\left( \begin{bmatrix} B_{X1} \\ B_{X2} \end{bmatrix}^T \left( \begin{bmatrix} B_{R1} & 0 \\ 0 & B_{R2} \end{bmatrix} \begin{bmatrix} P_{0R11} & P_{0R12} \\ P_{0R12}^T & P_{0R22} \end{bmatrix} \begin{bmatrix} B_{R1}^T & 0 \\ 0 & B_{R2}^T \end{bmatrix} + \begin{bmatrix} P_{TU1} & 0 \\ 0 & P_{TU2} \end{bmatrix} + \begin{bmatrix} \Sigma_1 & 0 \\ 0 & \Sigma_2 \end{bmatrix} \right)^{-1} \begin{bmatrix} B_{X1} \\ B_{X2} \end{bmatrix} \right)^{-1} . \quad (35)$$

The following are supporting definitions/computations:

$B_{Xj}$  is the  $2 \times 3$  matrix of partial derivatives of  $(l, s)$  with respect to  $X$  for image  $j$  in units of pixels/meter and evaluated at the *a priori* ground point location  $X_0 = 0.5 (i2g(l_1, s_1, z_0) + i2g(l_2, s_2, z_0))$  , where the *i2g* function (iterative inverse of RPC ground-to-image polynomial) is image dependent. (Note that the subscript in  $B_{Xj}$  corresponds to one ground point and one of two images, not one of two ground points and one image as in section 3.2 on monoscopic relative error propagation.) (36)

$B_{Rj}$  is the  $2 \times 2$  matrix of partial derivatives of  $(l, s)$  with respect to the baseline RPC adjustable parameters for image  $j$ . The units of  $B_{Rj}$  are pixels/pixels or unit-less, and  $B_{Rj} = I_{2 \times 2}, j = 1, 2$  . (37)

$P_{0Rjj}$  is the  $2 \times 2$  *a priori* error covariance matrix of the RPC adjustable parameters in units of pixels-squared for image  $j$ .  $P_{0Rjj} = eb_j^2 A_j A_j^T$  . (38)

The matrix  $A_j$  has units of pixels/meter and is computed as detailed in Section 2.4.1, with the exception that all *i2g* and *g2i* calls are via the RPC sensor model instead of the physical sensor model, and that image coordinates  $i_c$  and *a priori* elevation  $z_c$  , which correspond to the center of image  $j$ , are used instead of  $i_i$  and  $z_i$  corresponding to grid point  $i$ . (39)

$P_{OR12}$  is the  $2 \times 2$  *a priori* cross-covariance matrix of the RPC adjustable parameters for images 1 and 2, in units of pixels<sup>2</sup>.  $P_{OR12} = \rho \cdot eb_1 \cdot eb_2 \cdot A_1 A_2^T$ , where  $\rho = \text{cort}(\Delta t)$ , evaluated at the specific delta time  $\Delta t = |t_1 - t_2|$  between the two images. (40)

If a CSM plugin is available for RPC, the reference time for an image is via `getReferenceDateAndTime`. (If a CSM plugin is not available for RPC, use the physical sensor model CSM plugin instead. If neither are available, obtain the time directly from the corresponding NITF TRE.) Set  $t_j$  above to the reference time in seconds for image  $j$ ,  $j = 1, 2$ .

$P_{TUj}$  is the  $2 \times 2$  covariance matrix of total RPC unmodeled errors mapped to image space in units of pixels-squared for image  $j$ .  $P_{TUj} = er_j^2 A_j A_j^T$ . (41)

If a CSM plugin is available for RPC, the above  $P_{ORjj}$  is directly available via `getCurrentParameterCovariance`,  $P_{OR12}$  via `getCovarianceModel`,  $P_{TUj}$  via `getUnmodeledError`,  $B_{Xj}$  via `computeGroundPartials`, and  $B_{Rj}$  via `computeSensorPartials`, image  $j = 1, 2$ .

Following the computation of  $CovX$  (Equation 35), the following final computations are performed:

Convert  $CovX$  to a local tangent plane coordinate system representation:  $\rightarrow \Phi_{PtoL} CovX \Phi_{PtoL}^T$ , where  $\Phi_{PtoL}$  is applicable at the nominal location  $X_0$ . (42)

Compute  $CE$  and  $LE$  using , i.e.,  $CE = CE\{CovX\}$ ,  $LE = LE\{CovX\}$ . (43)

## 5.0 References

[1] Dolloff, J., Replacement Sensor Models, Chapter 11.3, *Manual of Photogrammetry*, Fifth Edition. J.C. McGlone editor. ASPRS, pp. 887-943, 2004.

[2] Dolloff, J., M. Iiyama, and C, Taylor, The Replacement Sensor Model (RSM): Overview, Status, and Performance Summary, ASPRS 2008 Annual Conference, Portland Oregon, April 28-May 2, 2008

[3] NTB, "NITF Technical Board, STDI-0002-1v4.0, Airborne Support Data Extensions". Appendix E, Table E-22, 2011; last accessed January 05, 2012;  
[http://www.gwg.nga.mil/ntb/baseline/docs/stdi0002/stdi0002\\_v40/index.html](http://www.gwg.nga.mil/ntb/baseline/docs/stdi0002/stdi0002_v40/index.html)

[4] Theiss, Hank, "Modification of CSM API to Support Stereo Image Pairs", CSMWG Meeting, Melbourne FL, 13 Jan 2010.

[5] Dolloff, J., Parameter Ranges for a Valid CSM Decay Model, white paper, Sensor Geospositioning Center, 06, July, 2010.

[6] Dolloff, J., Assembling a Multi-Imaging Event Error Covariance Matrix, white paper, Sensor Geopositioning Center, 06 July, 2010.

[7] BAE Systems (prepared for the NGA), Generic RPC Uncertainty Analysis Report, MSP Program, 04 October 2012, ITAR restricted.

[8] Iiyama, M., J. Dolloff, and C. Taylor, The ABCs of RSM: An Introduction to the Replacement Sensor Model, 30 September, 2006,  
<http://www.socetxp.com/content/products/special-products/replacement-sensor-model-rsm>

## **Appendix A: Comparison of Results: Physical versus RPC Sensor Model**

This appendix compares mono and stereo extraction and error propagation results based on the physical sensor model and based on the corresponding RPC sensor model. Both RPC uncertainty parameter generation and monoscopic and stereo extraction/error propagation are per the main body of this document.

REMAINDER OF THIS APPENDIX REMOVED IN THIS VERSION OF THE DOCUMENT  
AS CONSIDERED: *company sensitive*.

## **Appendix B: “Status of RPC Error Model, SGC, 14 March 2011” with Postscript**

### **Status of RPC Error Model**

**SGC, 14 March 2011**

This document provides a summary of the status of the RPC error model from a generator (CI vendor) and exploiter (tool vendor) standpoint, and some options for consideration. Let us begin by stating that an error model must be able to support uncertainty estimation for two main scenarios: 1) calculation of dimensions that involves measurements of multiple points in typically one image; and 2) extraction of absolute geolocation of target coordinates by measuring the point in one or more images. Let us term these scenarios “relative mensuration” and “target extraction”, respectively.

To allow both scenarios, three error terms are required in a simple-minded world where: 1) errors are categorized as either random or bias; 2) the imaging loci are essentially parallel at multiple pixel locations within an image, thereby eliminating perspective effects; and 3) error magnitudes are equal per-axis (e.g., circles instead of ellipses) and also assumed equal per same-pass image. Further note that these error terms correspond to support data errors only, not to random mensuration error due to an image work-station operator or an automatic correlator, which must be accounted for separately.

More specifically, the total support data error vector for a measured pixel location within an image, and with respect to WGS-84, is expressed as the sum of three error vectors (each vector with an expected value of zero and uncorrelated with the others):  $e_1$  = the component that is common to all images taken from the same orbital pass;  $e_2$  = the component that is common to all points that lie on the same image; and  $e_3$  = the component that is random for each point. Each of these components or error vectors is two-dimensional, i.e., has two elements or axes. The two elements in a given error vector are also assumed to have the same one-sigma uncertainties and are uncorrelated with each other.

Let  $s_1$ ,  $s_2$ , and  $s_3$  be defined as the one-sigma uncertainties per element (axis) associated with  $e_1$ ,  $e_2$ , and  $e_3$ , respectively. These three standard deviations can be considered sub-allocations of ERR\_BIAS and ERR\_RAND, heretofore termed  $e_b$  and  $e_r$ , respectively.  $e_b$  and  $e_r$  are contained in the RPC meta-data NITF tagged record extension, i.e., RPCB TRE. However, two communities or groups, the “relative mensuration group” and the “target extraction group”, essentially in isolation from each other, developed two different interpretations of  $e_b$  and  $e_r$  based on their particular interests or operational charters. These two interpretations also correspond to the two documents, STDI-0002 and NNDDD.

The target extraction group was primarily interested in geolocating a single point at a time using one or two (same-pass) images. Hence, relative mensuration and isolating the random error at each point ( $s_3$  in the previous paragraphs) was irrelevant. They defined  $e_b = s_1$ , and  $e_r = r_{ss}(s_2, s_3) = \sqrt{s_2^2 + s_3^2}$ . Therefore, support data error corresponding to a pair of pixels, each in a different but same-pass image, is modeled as correlated between 0 to 100%, depending on the relative size of  $e_b$  and  $e_r$ . On the other hand, the support data error is modeled as 100% correlated for two pixels in the same image. The standard deviation of (total) support data error for an arbitrary pixel location equals  $r_{ss}(e_b, e_r)$ . Further note that the support data error statistics ( $e_b$  and  $e_r$ ) are assumed relative to a ground coordinate system perpendicular to the line-of-sight (image locus) vector, with expected magnitudes circular in this coordinate system.

The relative mensuration group was primarily interested in exploitation of a single image, typically involving simultaneous measurements of multiple points to obtain dimensions, e.g., runway length and/or width. In the cases that they performed stereo point extractions, they had no requirement for rigorous error propagation that would make them care about considering correlation between a pair of images and whether it would result in correct error propagation. (It is also likely that individuals within and between CI companies may also disagree about the degree to which same-pass images are correlated.)

In other words, the relative mensuration group never felt the need to isolate the  $s_1$  component of uncertainty. Hence, they defined  $e_b = \sqrt{s_1^2 + s_2^2}$ , and  $e_r = s_3$ . Therefore, the support data error corresponding to a pair of pixels, each in a different but same-pass image, is modeled as uncorrelated. The support data error for two pixels in the same image is modeled as correlated between 0 and 100%, depending on the relative size of  $e_r$  and  $e_b$ . The standard deviation of support data error for an arbitrary pixel location equals  $r_{ss}(e_b, e_r)$ . Further note that the support data error statistics ( $e_b$  and  $e_r$ ) are also assumed relative to a local tangent plane ground coordinate system, with expected magnitudes circular in this coordinate system.

Preliminary results by the SGC using real CI data shows that same-pass images are correlated approximately 70%; and the value obtained by evaluating temporal correlation functions used in CI-provided physical sensor models also yields approximately 70%. So if we had to choose between non-zero (target extraction group) or zero (relative mensuration group) temporal correlation between images, the former is a closer representation. (In fact, it can be made to match 70% or a more refined number based on future analyses.) Hence, the STDI-0002 document provides a more realistic definition of these error terms, namely that  $e_b$  represents non-zero correlation between images. However, correlation between two pixels in the same image remains 100%, a "short-coming" if one is interested in relative mensuration between two or more points in an image.

That being said, in 2002 John Dolloff had written a proposed algorithm that is an adaptation to the target extraction group's error model. It uses a database constant,  $K$ , which is used to split  $e_r$  into its  $s_2$  and  $s_3$  components. In this model, the  $e_b$  term remains the same, i.e. equal to  $s_1$ . The

correlation coefficient between a pair of same-pass images is then equal to  $s1*s1/(s1*s1 + s2*s2+s3*s3)$ . The correlation coefficient between two pixels in the same image is  $(s1*s1+s2*s2)/(s1*s1+s2*s2+s3*s3)$ . And, of course, the standard deviation of support data error at an arbitrary pixel location is equal to  $\sqrt{s1*s1+s2*s2+s3*s3}$ .

(Note:  $s3$  corresponds to random error, and hence, its corresponding error  $e3$  is not adjustable as part of an RPC adjustment model. Thus, it can be alternatively assigned to (a portion of) random mensuration error, i.e., not considered an explicit portion of sensor support data error and sometimes termed “unmodeled error”. If so,  $s3$  is not included in the formulas in the previous paragraph.)

An alternate but equivalent algorithm would involve adaptation of the relative mensuration group’s error model. It could use a database constant,  $Kb$ , to split the  $eb$  into its  $s1$  and  $s2$  components. In this model, the  $er$  term would remain the same, i.e. equal to  $s3$ . The correlation coefficient between a pair of same-pass images would then be equal to  $s1*s1/(s1*s1 + s2*s2+s3*s3)$ , the correlation coefficient between two pixels in the same image  $(s1*s1+s2*s2)/(s1*s1+s2*s2+s3*s3)$ , and the standard deviation of support data error at an arbitrary pixel location is equal to  $\sqrt{s1*s1+s2*s2+s3*s3}$  - the same as the 2002 Dolloff algorithm for the target extraction group’s error model.

Since we cannot add another field/number to the RPCB TREs, the value of the database constant ( $K$  or  $Kb$ ) would have to be made known to all CI vendors and all tool vendors, and could also vary per sensor. Furthermore, a specific algorithm would need to be extensively documented in order to explain how to generate and how to exploit the error terms. In addition, the SGC recommends that the  $eb$  and  $er$  statistics should be relative to a common coordinate system for both groups’ error models. The ground coordinate system is perpendicular to the line-of-sight or imaging-locus, not the local tangent plane.

\*\*\*\*\*

### **Status of RPC Error Model: Postscript**

**SGC, July 2011**

Further analyses indicate that the relative variability of temporal correlation of systematic errors between same-pass images is much less than the relative variability of the magnitude of total unmodeled error for an image. By relative variability, we mean variability from image to image. (Temporal correlation affects target extraction and unmodeled or random error primarily affects relative mensuration.)

Thus, it follows that the basic design should be consistent with the “relative mensuration camp”. In particular,  $eb$  corresponds to RPC error considered systematic (a bias) across the image, and  $er$

corresponds to RPC error considered uncorrelated (random) across the image. That is, using earlier notation,  $e_b = \sqrt{s_1^2 + s_2^2}$ , and  $e_r = s_3$ .

However, there is an addition to the above design commensurate with the requirements of the “target extraction camp”: Temporal correlation of RPC systematic error between images will be available. It will be represented by a pre-computed correlation function and published by the image vendor per sensor. (This is actually a generalization of a pre-computed correlation coefficient value as represented by either a data base parameter K or K<sub>b</sub>, discussed above in the “Status of RPC Error Model, SGC, 14 March 2011”.)

There is also another addition along these same lines that provides for higher fidelity representation of RPC intra-image errors in order to further support the “relative mensuration error camp”. A correlation function for RPC total unmodeled errors will be available, also published by the image vendor per sensor. It is a function of delta-line and delta-sample between two points in the same but arbitrary image. This function allows for the representation of higher relative accuracy between two points closer together than for two points farther apart.

Both the above correlation functions are to be rarely changed by the vendor and are described further in Appendix G.

The remaining design issue was which ground plane should RPC uncertainty parameters reference – the local horizontal tangent plane (“LTP”) or a plane perpendicular to the image line-of-sight vector (“PER”)?. The “firm” conviction that “PER” was the best choice indicated earlier in “Status of RPC Error Model, SGC, 14 March 2011” was reconsidered and a trade-study performed (see Appendix K). It indicated that “LTP” is a slightly better choice considering the relative benign nature of commercial satellite imaging (imaging angles).

The above overall design presented in this “Postscript” is reflected in the main body of this document. That is, in both in both the generation and the application of RPC uncertainty parameters.

Finally, the two interpretations of the RPCB TRE discussed earlier in “Status of RPC Error Model, SGC, 14 March 2011” are presented in detail in Appendix C. The actual fields and formats are the same for the two interpretations; however, the corresponding descriptions of the uncertainty parameters differ. For the recommended SGC design, their proper definition is as above in this “Postscript”, and in conjunction with the published correlation functions not explicitly contained in the TRE.

## Appendix C: RPC00B TRE Description

The following excerpt describes the relevant portions of the RPCB (RPC00B) TRE – see [3] for the latest and entire TRE. It corresponds to STDI-0002, and correspondingly, to the “target extraction group” interpretation discussed earlier in Appendix B.

(The NNDDD presents the RPCB TRE that corresponds to the “relative mensuration group” interpretation, where eb (ERR\_BIAS) is assumed to correspond to uncorrelated images.)

-----Excerpt-----

# NITF Compendium STDI-0002 v3

## E.3.12 RPC00 - Rapid Positioning Capability

RPC00 contains rational function polynomial coefficients and normalization parameters that define the physical relationship between image coordinates and ground coordinates. Use of RPC00 is optional. The format and descriptions for the user-defined fields of the RPC00B extension is detailed in table E-22. A discussion of the polynomial functions is contained in Section E.2.4. Note that the order of terms in the polynomial in RPC00B is different from RPC00A (defined in STDI-0001).

E-74

**Table E-22. RPC00B - Rapid Positioning Capability Extension Format**

R = REQUIRED, C = CONDITIONAL, <> = BCS SPACES ALLOWED FOR ENTIRE FIELD

FIELD	NAME/DESCRIPTION	SIZE	VALUE RANGE	UNITS	TYPE
CETAG	Unique Extension Identifier.	6	RPC00B		R
CEL	Length of Entire Tagged Record.	5	01041	bytes	R
<i>The following fields define RPC00B</i>					
SUCCESS		1	1		R
ERR_BIAS	Error - Bias. 68% non time-varying error estimate assumes correlated images.	7	0000.00 to 9999.99	meters	R
ERR_RAND	Error - Random. 68% time-varying error estimate assumes uncorrelated images.	7	0000.00 to 9999.99	meters	R
LINE_OFF	Line Offset	6	000000 to 999999	pixels	R

## Appendix D: Unmodeled Errors

Unmodeled errors consist of errors that cannot be practically characterized by (errors in) the physical sensor model's image support data adjustable parameters. They consist of:

- (1) High frequency variations in (true) image support data associated with the exterior orientation of the sensor; inherent with the imaging system and/or due to interpolation error of the (*a priori*) image support data provided as part of the physical sensor model.
- (2) *A priori* image support data interior orientation errors, such as chip alignment errors.
- (3) Errors resultant from mapping the representation of image support data adjustable parameters from a higher fidelity set to a lower fidelity set for the physical sensor model, when applicable.

Total unmodeled error includes the above plus RPC polynomial fit error relative to the physical sensor model's  $g2i$  function.

For the generation of RPC uncertainty parameters, total unmodeled errors are uncorrelated between images but can be correlated between two different locations within the same image, as specified by the vendor supplied correlation function  $corp(\Delta l, \Delta s)$  detailed in Appendix G. For example, we expect that polynomial fit error has a common component at two locations within the same image a relatively short distance apart. Thus, we expect correlation to be higher than for two locations far apart in the image – say a correlation of 0.7 versus 0.0. Correspondingly, relative accuracy will be higher (better) when the two points are close together; for example, corresponding to two points at the ends of a feature of interest with a dimension on the order of 25 meters.

## Appendix E: Conversion of the Physical Sensor Model: Unrectified to Rectified Image

This appendix describes how to convert a physical sensor model relative to an unrectified (original) image to a physical sensor model relative to a rectified image. In the following, we use the superscript \* to represent scalars, vectors, matrices, and functions associated with the physical sensor model for the rectified image.

Let  $f(i)$  map the  $2 \times 1$  unrectified image coordinates  $i = (l \ s)^T$  to the  $2 \times 1$  rectified image coordinates  $i^* = (l^* \ s^*)^T$ , i.e.,  $i^* = f(i)$ . We assume that the function  $f(i)$  is given. Note that this function is two-dimensional; in particular, a two-dimensional output given a two-dimensional input.

Also, given the original ground-to-image function  $i = g2i(X)$ , we have  $i^* = g2i^*(X) = f(g2i(X))$ .

The image-to-ground function for the rectified image is  $i^*2g$  and is defined as the iterative inverse of  $g2i^*$ .

Define the  $2 \times 2$  matrix  $D_j$  as the partial derivatives of  $i^*$  with respect to  $i$  corresponding to ground point  $j$ , i.e., the partial derivative of  $f(i)$  with respect to  $i$  evaluated at the appropriate operating point (value of  $i$  corresponding to ground point  $j$ ).

Given the original  $2 \times 3$  matrix  $B_{Xj}$  of partial derivatives of  $i$  with respect to ground location  $X$  corresponding to ground point  $j$ , the  $2 \times 3$  matrix of partial derivatives of  $i^*$  with respect to  $X$  is  $B_{Xj}^* = D_j B_{Xj}$ .

The physical sensor model's adjustable parameters and their error covariance are identical for the two images. Therefore:

Given the original  $2 \times n$  matrix  $B_{Sj}$  of partial derivatives of  $i$  with respect to physical sensor model adjustable parameters  $S$  corresponding to ground point  $j$ , the  $2 \times n$  matrix of partial derivatives of  $i^*$  with respect to physical sensor model adjustable parameters  $S$  is  $B_{Sj}^* = D_j B_{Sj}$ .

In addition, given the original  $2 \times 2$  unmodeled error covariance corresponding to ground point  $j$  and  $2 \times 2$  unmodeled error cross-covariance between ground points  $j$  and  $k$ ,  $P_{Uj}$  and  $P_{Ujk}$ , respectively, the corresponding matrices with respect to rectified image coordinates are  $P_{Uj}^* = D_j P_{Uj} D_j^T$  and  $P_{Ujk}^* = D_j P_{Ujk} D_k^T$ , respectively.

Note: In the above, we are addressing rectified imagery, not ortho-rectified imagery. As such, for rectified imagery, an additional effect due to elevation uncertainty is not included in RPC

uncertainty parameter generation. The generation process is implemented exactly as documented in Section 2, using the physical sensor model described above. Also, elevation uncertainty is automatically accounted for in monoscopic extraction, exactly as documented in Section 3.

## Appendix F: Evaluation of *CE* and *LE*

The appendix describes the procedure to compute the scalar 0.9p circular error value *CE* and related statistical metrics. The procedure is relatively simple and fast.

Evaluate the function  $CE\{Cov\}$ , where the argument *Cov* is a 2x2 covariance matrix:

Determine the two eigenvalues of *Cov*. Compute *r* equal to the square root of the ratio of the smallest eigenvalue to largest eigenvalue. Interpolate *r* into a predetermined table (see below) to obtain a scale factor *k*. *CE* equals *k* times the square root of the largest eigenvalue.

<i>r</i>	0	.05	.10	.15	.20	.25	.30	.35	.40	.45	.50
<i>k</i>	1.64	1.65	1.65	1.65	1.66	1.67	1.67	1.69	1.70	1.72	1.74
<i>r</i>	.55	.6	.65	.70	.75	.80	.85	.90	.95	1.0	
<i>k</i>	1.76	1.79	1.83	1.86	1.90	1.95	1.99	2.04	2.09	2.15	

The above table was generated by numerically solving the following equation for *k* over a range of values for *r*:

$$p = 0.9 = \frac{1}{2\pi} \iint_{\sqrt{x^2+r^2y^2} \leq k} e^{-1/2(x^2+y^2)} dx dy$$

The equation was derived assuming a mean-zero Gaussian (normal) joint distribution of errors and using eigenvector/eigenvalue analysis (*Cov* becomes a diagonal matrix with eigenvalues on the diagonals when transformed to an eigenvector aligned coordinate system).

Note that when *CE* is to correspond to 0.9p horizontal error and we are given *CovX*, the 3x3 ground point error covariance matrix in local tangent plane coordinates, simply set *Cov* to the upper left 2x2 of *CovX* and proceed as above.

We can also compute *LE* which corresponds to 0.9p vertical error as follows using the lower right 1x1 of *CovX*:  $LE\{CovX\} = 1.64 (CovX(3,3))^{1/2}$ .

## Appendix G: Generation of Correlation Functions

This appendix details the functional form of the correlation functions  $cort(\Delta t)$  and  $corp(\Delta l, \Delta s)$ , the recommended method for their generation by the image vendors, and various examples.

### General Functional form

Both the temporal correlation function  $cort(\Delta t)$  and the pixel location correlation function  $corp(\Delta l, \Delta s)$  are represented by “CSM four parameter” correlation functions. A general “CSM four parameter” function is specified by the values of four parameters  $\{A, \alpha, \beta, T\}$  as follows:

$$\rho(\Delta t) = A \left[ \alpha + \frac{(1-\alpha)(1+\beta)}{\beta + e^{\Delta t/T}} \right] \quad (G1)$$

(The above assumes that the correlation function  $\rho(\Delta t)$  is a temporal correlation function for convenience, i.e., a function of  $\Delta t \geq 0$ , the absolute value of the time difference between two images.)

There are also restrictions on the ranges of the four parameters such that the correlation function is valid, i.e., a strictly positive definite correlation function (spdcf):

$$0 < A \leq 1, 0 \leq \alpha < 1, 0 \leq \beta \leq 10, \text{ and } 0 < T. \quad (G2)$$

Also,  $\rho(\Delta t = 0) \equiv 1$ ,  $\rho(\Delta t = 0 + \epsilon) = A$ , where  $\epsilon$  is an arbitrarily small positive number, and  $\rho(\Delta t \rightarrow \infty) = A\alpha$ , where  $A\alpha$  is the function’s “floor” value.

(An exception to the ranges in equation G2 is that  $\alpha = 1$  is also allowed if  $A < 1$ .)

Note that a value of  $A < 1$  corresponds to a stochastic process that includes a totally random (white noise) component, and a value of  $\alpha > 0$  corresponds to a stochastic process with a strictly bias component.

The following figure presents typical examples corresponding to  $A=1$  and  $\alpha = 0$ :

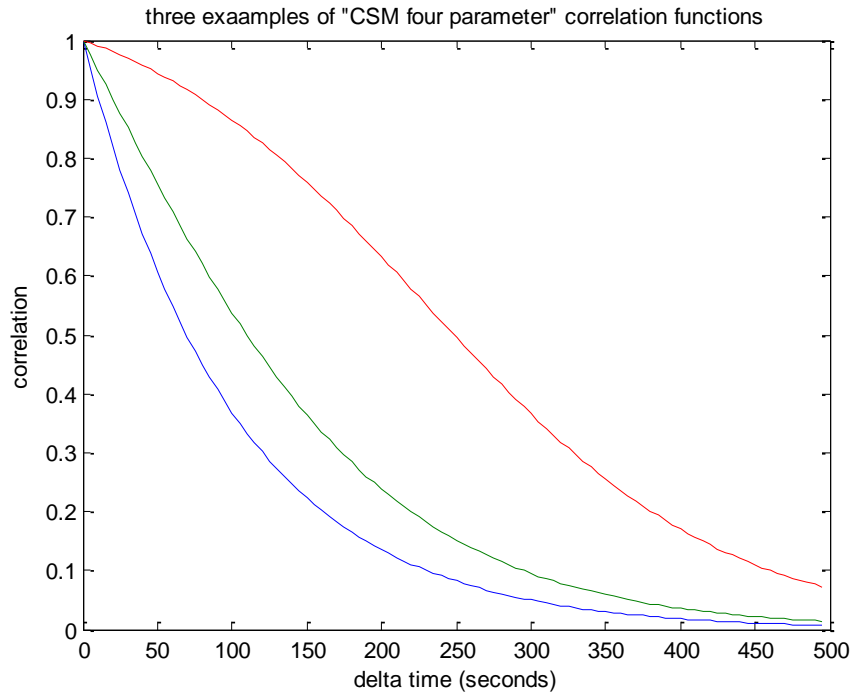


Figure G-1: Examples of “CSM four parameter correlations functions (A=1; alpha=0; beta =0, 1, and 10; T=100 sec)

See References [4]-[5] for more detail on the “CSM four parameter” correlation function. See Reference [6] for further information on spdcf and imagery-based applications.

Note: the above references use a slightly different form for the CSM four parameter correlation function than the form of Equation G1. The former form is compatible with the CSM 2.A version of the API, whereas the form of Equation G1 is compatible with CSM 3.0.1 version of the API. For completeness, the former form is presented as follows:  $\rho(\Delta t) = \alpha + A \frac{(1-\alpha)(1+\beta)}{\beta + e^{\Delta t/\tau}}$ , with valid parameter ranges identical to those corresponding to form G1.

### Temporal correlation function

$cort(\Delta t)$  has the functional form of Equation G1, and is specified by the values of the four parameters  $\{A, \alpha, \beta, T\}$ . The independent variable  $\Delta t$  is the absolute value of the time difference between two images on the same pass.

The effect of temporal correlation of errors on stereo error propagation is significant – see Table A-11 of Appendix A for examples.

The image vendor should generate  $cort(\Delta t)$  by considering the “CSM four parameter” correlation functions associated with the underlying physical sensor model’s adjustable

parameters. There can be multiple correlation functions associated with the physical sensor model, one for each independent (uncorrelated) group of adjustable parameters. If one such group is dominant, i.e., dominates the overall physical sensor model uncertainty, then  $cort(\Delta t)$  may simply be defined as that group's correlation function. For example, for some commercial satellite sensors, the group of attitude adjustable parameters may dominate.

However, if more than one group of physical sensor model adjustable parameters are relevant, then  $cort(\Delta t)$  should be defined based on a weighted average of the corresponding correlation functions. For example:

$$\rho(\Delta t) = (\sum_{i=1}^m Tr\{B_{Si} P_{Si} B_{Si}^T\})^{-1} \sum_{i=1}^m Tr\{B_{Si} P_{Si} B_{Si}^T\} \rho_{Si}(\Delta t), \quad (G3)$$

where  $i$  corresponds to the subgroup, and  $P_{Si}$ ,  $B_{Si}$ , and  $\rho_{Si}$  the corresponding error covariance, partial derivative matrix of image coordinates with respect to the adjustable parameters, and the "CSM four parameter" correlation function, respectively, for subgroup  $i$  and for a typical image for the relevant sensor. ( $Tr\{\}$  is the matrix trace.)

$\rho(\Delta t)$  in Equation G3 defines a function, but not necessarily of the correct form. Thus, the actual RPC correlation  $cort(\Delta t)$  is defined by the values of four parameters ( $A, \alpha, \beta, T$ ) determined by their best fit to  $\rho(\Delta t)$ .

#### Default values

If the four parameters defining the temporal correlation function are not available (published by the appropriate vendor), their default values are as follows for WorldView and GeoEye imagery:

WorldView -  $\{A, \alpha, \beta, T\} = \{1, 0, 10, 37 \text{ sec}\}$

GeoEye -  $\{A, \alpha, \beta, T\} = \{1, 0, 10, 42 \text{ sec}\}$ .

Note that for typical delta time between stereo images on the same pass, the above yield an approximate correlation value of  $cort(\Delta t) = 0.7$ , or 70%. Also, the above default values are independent of the particular function form for the temporal correlation function (compatible with either CSM 2.A or CSM 3.0.1) since  $A = 1$  and  $\alpha = 0$ .

Reference [7] provides further insight into these default values and their effect on error propagation (accuracy prediction).

#### Pixel location correlation function

$corp(\Delta l, \Delta s)$  is defined as the product of two "CSM four parameter" correlation functions, one a function of the absolute value of delta-line ( $\Delta l$ ), and the other a function of the absolute value of delta-sample ( $\Delta s$ ):

$$corp(\Delta l, \Delta s) = corpl(\Delta l) \cdot corps(\Delta s) \quad (G4)$$

The two sets of four parameters  $\{A, \alpha, \beta, T\}$  that define  $corp(\Delta l, \Delta s)$ , one set corresponding to  $corpl(\Delta l)$  and the other to  $corps(\Delta s)$ , are to be computed such that  $corp(\Delta l, \Delta s)$  approximates the correlation of RPC total unmodeled error between two pixel locations in the same image. This error is the sum of two errors, unmodeled error and RPC polynomial fit error. Unmodeled error is associated with the underlying physical sensor model.

Thus, the vendor should determine  $corp(\Delta l, \Delta s)$  by taking the weighted average of a pair of correlation functions. These two functions are defined as follows and are also represented by “CSM four parameter” correlation functions:

(1)  $corp\_um(\Delta l, \Delta s) = corpl\_um(\Delta l) \cdot corps\_um(\Delta s)$ , corresponding to the physical sensor model’s unmodeled error, and

(2)  $corp\_pf(\Delta l, \Delta s) = corpl\_pf(\Delta l) \cdot corps\_pf(\Delta s)$ , corresponding to polynomial fit error for both a typical image and the image vendor’s polynomial fit process.

The vendor must first determine both  $corp\_um(\Delta l, \Delta s)$  and  $corp\_pf(\Delta l, \Delta s)$  and then weight them by the expected variance of error associated with both error processes:

$$\rho(\Delta l, \Delta s) = \frac{\sigma_{pf}^2 corp\_um(\Delta l, \Delta s) + \sigma_{um}^2 corp\_pf(\Delta l, \Delta s)}{\sigma_{um}^2 + \sigma_{pf}^2} \quad (G5)$$

$\rho(\Delta l, \Delta s)$  in Equation G5 defines a function, but not necessarily of the correct form. Thus, the actual correlation function  $corp(\Delta l, \Delta s) = corpl(\Delta l) \cdot corps(\Delta s)$  is determined by the values of two set of four parameters  $(A, \alpha, \beta, T)$  determined by their best fit to  $\rho(\Delta l, \Delta s)$ .

(Note that the fidelity of the vendor-published  $corp(\Delta l, \Delta s)$  is dependent of the applicability of the *a priori* weighting of  $corp\_um(\Delta l, \Delta s)$  and  $corp\_pf(\Delta l, \Delta s)$ , i.e., on the relative invariance of the *a priori* unmodeled error variance to the *a priori* polynomial fit error variance across images.)

Generation and use of  $corp(\Delta l, \Delta s)$  allows for better relative error (high positive correlation) at two locations close together in the same image as opposed to two locations far apart (low positive or zero correlation) in the same image. Its form as a product of two correlation functions, one a function of delta-line and the other delta-sample, allows for different correlation characteristics in the two directions.

The following is a simple hypothetical example of a correlation function  $corp$  based on the assumptions:

(1) unmodeled errors are uncorrelated across the image, i.e.,  $corp\_um(\Delta l, \Delta s) = 0$

(2) a 2:1 ratio of polynomial fit (one-sigma) errors to unmodeled (one-sigma) errors

$$(3) \text{corp\_pf}(\Delta l, \Delta s) = e^{-\Delta l/2000} \cdot e^{-\Delta s/1000}$$

$$(4) \text{corp}(\Delta l, \Delta s) = \left(\frac{2^2}{1^2+2^2}\right) \text{corp\_pf}(\Delta l, \Delta s) + \left(\frac{1^2}{1^2+2^2}\right) \text{corp\_um}(\Delta l, \Delta s) =$$

$$(0.8)e^{-\Delta l/2000} \cdot e^{-\Delta s/1000} + 0 = ((0.8^{1/2})e^{-\Delta l/2000}) \cdot ((0.8^{1/2})e^{-\Delta s/1000})$$

(5) the corresponding sets of 4 parameters  $\{A, \alpha, \beta, T\}$  that specify  $\text{corp}(\Delta l, \Delta s)$  are  $\{\text{sqrt}(0.8), 0, 0, 2000\}$  and  $\{\text{sqrt}(0.8), 0, 0, 1000\}$

Figure G-2 plots  $\text{corp}(\Delta l, \Delta s)$ :

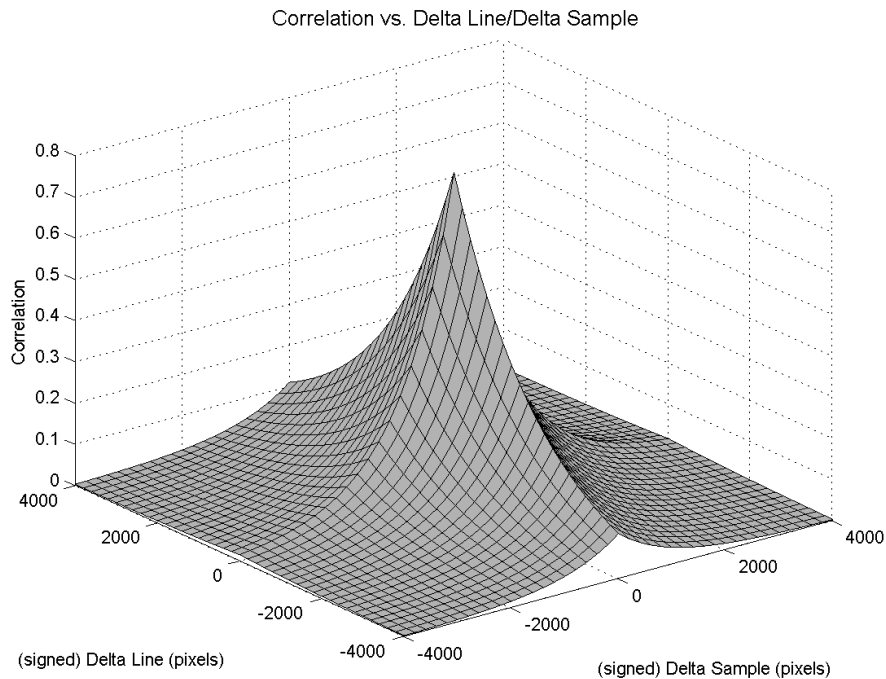


Figure G-2: Example of  $\text{corp}(\Delta l, \Delta s)$

In order to examine the approximate effect of  $\text{corp}(\Delta l, \Delta s)$  on monoscopic relative error propagation, we consider only the effects of the  $4 \times 4$  total unmodeled error covariance matrix

$\begin{bmatrix} P_{TU1} & P_{TU12} \\ P_{TU12}^T & P_{TU2} \end{bmatrix}$  in Equation (23) for  $CovX$  in the main body of this document. That is, we

realistically assume that the effects of RPC systematic error are small, and that unmodeled error dominates mensuration error at the two locations. We further assume for simplicity that image coordinates map directly to horizontal ground coordinates.

Finally, we assume that the  $2 \times 2$  diagonal blocks ( $P_{TU1}$  and  $P_{TU2}$ ) of the total unmodeled error covariance correspond to diagonal matrices with 1 meter-squared down the diagonals ( $er=1$ ), and that the  $2 \times 2$  cross-block ( $P_{TU12}$ ) is computed using the specific  $\text{corp}(\Delta l, \Delta s)$  presented above.

Corresponding relative horizontal CE is presented in Figure G-3. Note the improved relative accuracy (smaller CE) for two points close together in the same image.

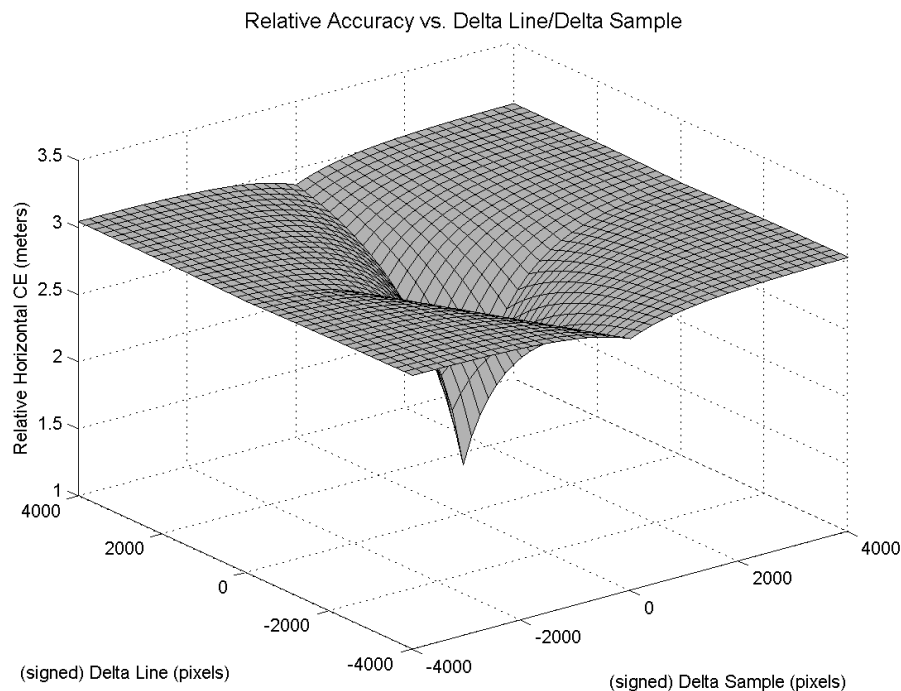


Figure G-3: Example of the Effect of  $corp(\Delta l, \Delta s)$  on Relative Accuracy

### Default values

If the two sets of four parameters defining the pixel location correlation function are not available (published by the appropriate vendor), their default values (to be refined) are as follows for both WorldView and GeoEye imagery:

$\{A, \alpha, \beta, T\}$ -line =  $\{1, 0, 10, 200 \text{ pixels}\}$ -line;  $\{A, \alpha, \beta, T\}$ -sample =  $\{1, 0, 10, 2000 \text{ pixels}\}$ -sample.

Note that the above yield a (combined) approximate correlation value of  $corp(\Delta l, \Delta s) = 0.99$  for  $(\Delta l, \Delta s) = (20 \text{ pixels}, 20 \text{ pixels})$ , and  $corp(\Delta l, \Delta s) = 0.60$  for  $(\Delta l, \Delta s) = (400 \text{ pixels}, 400 \text{ pixels})$ .

The default values assume higher correlation of error in the sample (cross-scan) direction.

Also, the above default values are independent of the particular function form for the pixel location correlation function (compatible with either CSM 2.A or CSM 3.0.1) since  $A = 1$  and  $\alpha = 0$ .

Reference [7] provides further insight into some of these default values and their effect on error propagation (accuracy prediction).

## Appendix H: Ancillary Stereo Computations

This appendix discusses: (1) the complete WLS solution for stereo images, (2) an RPC adjustment model with more adjustable parameters than the baseline set, and (3) miscellaneous comments concerning equivalences, approximations, and use of a previously adjusted RPC sensor model, i.e., the use of *a posteriori* RPC adjustable parameter values and corresponding error covariance.

### Complete WLS solution

Section 4.4 presented error propagation equations only, i.e., the computation of  $CovX$  for stereo imagery. The following presents the integrated complete weighted least squares (WLS) solution which includes the best estimate of the ground point location  $X$  and the corresponding error covariance  $CovX$ . (The equation for  $CovX$  presented here is equivalent to that presented in the main body of the document.) Although not presented here, the solution ( $X$  and  $CovX$ ) is typically iterated about a (new) operating point (*a priori* ground location  $X_0$ ). The following utilizes the notation previously defined in Section 4 as well as some generalizations.

Define the  $4 \times 4$  measurement weight matrix as:

$$W = \left( \begin{bmatrix} B_{R1} & 0 \\ 0 & B_{R2} \end{bmatrix} \begin{bmatrix} P_{0R11} & P_{0R12} \\ P_{0R12}^T & P_{0R22} \end{bmatrix} \begin{bmatrix} B_{R1}^T & 0 \\ 0 & B_{R2}^T \end{bmatrix} + \begin{bmatrix} P_{TU1} & 0 \\ 0 & P_{TU2} \end{bmatrix} + \begin{bmatrix} \Sigma_1 & 0 \\ 0 & \Sigma_2 \end{bmatrix} \right)^{-1}$$

Define the  $2 \times 1$  *a priori* measurement residual vector as:

$Z_j = M_j - \hat{M}_j$ ,  $j = 1, 2$ , and where the  $2 \times 1$  vector  $\hat{M}$  corresponds to the predicted measurement corresponding to the *a priori* ground location  $X_0$ , i.e.,  $\hat{M}_j = g2i(X_0)$ , and the  $2 \times 1$  vector  $M_j$  is the actual measurement, i.e.,  $M_j = i_j = [l_j \quad s_j]^T$ .

Concatenate the partial derivative matrices and residual vectors as follows for convenience:

$$B_X = \begin{bmatrix} B_{X1} \\ B_{X2} \end{bmatrix} \text{ and } Z = \begin{bmatrix} Z_1 \\ Z_2 \end{bmatrix}.$$

The complete weighted least squares solution is:

$$CovX = (B_X^T W B_X)^{-1}$$

$$\hat{X} = X_0 + (CovX) B_X^T W Z.$$

(Note: the above complete stereo solution is easily extended to a simultaneous solution for multiple ground points, but not detailed here.)

(Note: of course, for mono extraction, the best estimate or weighted least squares solution  $\hat{X}$  for the ground point is simply the output of the  $i2g$  function. This is also true for simultaneous extraction of multiple ground points in the same image.)

### Additional RPC adjustable parameters

If there is an RPC adjustment model that includes more than image offsets (one in the line direction and one in the sample direction), the above WLS solution for the ground point's location and corresponding error covariance can be modified appropriately. (However, image offsets alone are generally preferred for WLS (target extraction) solutions, whether corresponding to mono or stereo extractions.)

Let us assume that the RPC adjustable parameters also include rate terms. We also assume for simplicity that the RPC model has not been previously adjusted by a down-stream adjustment process after its initial generation; thus, values for the RPC adjustable parameters are zero.

(The following equations also serve to define the values output via a corresponding RPC CSM plugin. In addition, they serve as a roadmap or guideline for implementation of an adjustment process for the RPC, i.e., to a registration or "triangulation" which computes non-zero values for the RPC adjustable parameters. The addition of rate terms is generally preferred for an adjustment process.)

Define the RPC adjustable parameters for an image as the components in the vector =  $[a_0 \ b_0 \ a_1 \ b_1 \ a_2 \ b_2]^T$ , and where their effects on image coordinates is as follows:

$$\Delta l = a_0 + a_1 l' + a_2 s'$$

$$\Delta s = b_0 + b_1 l' + b_2 s' .$$

$l', s'$  are normalized image coordinates ranging in value from -1 to +1 across the image in the line and sample directions, respectively. The units for all six adjustable parameters is pixels.

Define the  $2 \times 6$  matrix of partial derivatives of image coordinates with respect to the RPC adjustable parameters for image  $j$  as follows:

$$B_{Rj} = \begin{bmatrix} 1 & 0 & l' & 0 & s' & 0 \\ 0 & 1 & 0 & l' & 0 & s' \end{bmatrix}.$$

Define the  $6 \times 6$  RPC *a priori* error covariance matrix with respect to the RPC adjustable parameters for each image  $j = 1,2$  as:

$$P_{ORjj} = E\{\varepsilon R_j \varepsilon R_j^T\} = eb_j^2 \begin{bmatrix} A_j A_j^T & 0 & 0 \\ 0 & f^2 A_j A_j^T & 0 \\ 0 & 0 & f^2 A_j A_j^T \end{bmatrix}, \text{ where}$$

$A_j$  is the previously defined  $2 \times 2$  matrix of partial derivatives of image coordinates with respect to horizontal ground plane coordinates at the center of the image. The parameter  $f$  allocates a portion of RPC uncertainty to the rate terms, while leaving the allocation to the offset terms unchanged. This leaves the *a priori* absolute uncertainty at the center of the image unchanged, but increases *a priori* absolute uncertainty (somewhat pessimistic) at the ends of the image. Also, due to the addition of the rate terms ( $f > 0$ ), *a priori* relative uncertainty corresponding to two arbitrary points in the same image increases with distance between the points. A recommended default value for  $f$  is 0.25. (Note that both  $f$  and the default value for  $cort(\Delta t)$  should be specifiable data base parameters.)

Define the  $6 \times 6$  RPC *a priori* error cross-covariance matrix with respect to the RPC adjustable parameters between the two images as:

$$P_{R12} = E\{\varepsilon R_1 \varepsilon R_2^T\} = \rho eb_1 eb_2 \begin{bmatrix} A_1 A_2^T & 0 & 0 \\ 0 & f^2 A_1 A_2^T & 0 \\ 0 & 0 & f^2 A_1 A_2^T \end{bmatrix}, \rho = cort(\Delta t).$$

Note that the full two-image RPC adjustable error covariance  $P = \begin{bmatrix} P_{OR11} & P_{OR12} \\ P_{OR21} & P_{OR22} \end{bmatrix}$  is a valid  $12 \times 12$  covariance matrix. In particular, there are three groups of uncorrelated adjustable parameters: line and sample offset, line and sample rates with respect to normalized line, and line and sample rates with respect to normalized sample. Each of these groups references four adjustable parameters, two for each image, and each of these groups has a valid  $4 \times 4$  sub-covariance in  $P$ . As an example, the sub-covariance for the line and sample offsets is equal to:

$$P_{ls\ sub} = \begin{bmatrix} eb_1^2 A_1 A_1^T & \rho eb_1 eb_2 A_1 A_2^T \\ \rho eb_1 eb_2 A_2 A_1^T & eb_2^2 A_2 A_2^T \end{bmatrix} = \begin{bmatrix} A_1 & 0 \\ 0 & A_2 \end{bmatrix} \begin{bmatrix} eb_1^2 I_{2 \times 2} & \rho eb_1 eb_2 I_{2 \times 2} \\ \rho eb_1 eb_2 I_{2 \times 2} & eb_2^2 I_{2 \times 2} \end{bmatrix} \begin{bmatrix} A_1 & 0 \\ 0 & A_2 \end{bmatrix}^T$$

which is clearly a valid covariance matrix since the  $A_j$  have full rank 2 and the correlation value is assumed via a strictly positive definite correlation function. Thus, a valid  $4 \times 4$  covariance matrix is pre and post multiplied by a full rank 4 transformation matrix and its transpose, respectively, which yields a positive definite and symmetric matrix, i.e. a valid  $4 \times 4$  covariance matrix  $P_{ls\ sub}$ .

The  $4 \times 4$  image measurement weight matrix is then defined as the inverse of the total image error covariance due to the combined effects of RPC adjustable parameter uncertainty, RPC total unmodeled error, and image mensuration error for both sets of image coordinates:

$$W = \left( \begin{bmatrix} B_{R1} & 0 \\ 0 & B_{R2} \end{bmatrix} \begin{bmatrix} P_{0R11} & P_{0R12} \\ P_{0R12}^T & P_{0R22} \end{bmatrix} \begin{bmatrix} B_{R1}^T & 0 \\ 0 & B_{R2}^T \end{bmatrix} + \begin{bmatrix} P_{TU1} & 0 \\ 0 & P_{TU2} \end{bmatrix} + \begin{bmatrix} \Sigma_1 & 0 \\ 0 & \Sigma_2 \end{bmatrix} \right)^{-1} .$$

The complete wls solution is:

$$CovX = (B_X^T W B_X)^{-1}$$

$$\hat{X} = X_0 + (CovX) B_X^T W Z .$$

### Equivalences, approximations, and *a posteriori* data

Note that when only two RPC adjustable parameters, line offset and sample offset, the above computation for  $CovX$  is equivalent to that presented in Equation (35) in the main body of this document which corresponds to the baseline RPC adjustment model.

Further note that there is an alternate form for  $P_{0R12}$ , regardless the number of RPC adjustable parameters:  $P_{0R12} = \rho P_{0R11}^{1/2} P_{0R22}^{T/2}$ , where the superscript  $1/2$  indicates matrix (principal) square root. However, this can yield different results than the form presented above if  $A_1$  differs significantly (e.g., in sign sense) from  $A_2$ . (Recall that  $P_{0Rjj} = e b_j^2 A_j A_j^T$ .) This is because, in general,  $(A_j A_j^T)^{1/2} \neq A_j$  and  $(A_1 A_1^T)^{1/2} (A_2 A_2^T)^{T/2} \neq A_1 A_2^T$ . However, the alternate form should yield very similar results if the line/sample directions for the two images are approximately aligned geographically; in which case,  $A_1 \cong A_2$ , and  $(A_1 A_1^T)^{1/2} (A_2 A_2^T)^{T/2} \cong A_1 A_2^T$ . (This is confirmed in Table K-2 of Appendix K.)

Finally, note that all the above WLS solutions in this appendix assume that the RPC sensor model is unadjusted, i.e., a “downstream” RPC registration/triangulation has not been performed previously. If it had, all the general equations are still applicable; however, the predicted measurements are first adjusted based on the non-zero values of the RPC adjustable parameters, and the RPC adjustable parameter error covariance is an *a posteriori* error covariance from the registration/triangulation process, not an *a priori* error covariance.

## Appendix I: Calculation of non-baseline x\*-y\* directions

This appendix presents the calculations of the x\*-y\* directions and corresponding A matrix for a ground plane perpendicular to the line-of-sight vector instead of the baseline horizontal ground plane. If one were to implement this method in order to represent RPC uncertainty, all of the previous generation and extraction/algorithms presented in the main body of this document do not change, other than calculation and use of this new A matrix.

### Generation and mono error propagation

The following matrix is defined as the 2x2 partial derivative matrix of image coordinates with respect to ground plane coordinates for grid point *i*. The ground plane is perpendicular to the image line-of-sight vector.

$$A_i \triangleq \frac{\partial(l_i, s_i)}{\partial(x_i^*, y_i^*)} \tag{11}$$

The x\* - y\* plane corresponding to an arbitrary grid point is illustrated in the following Figure I-1:

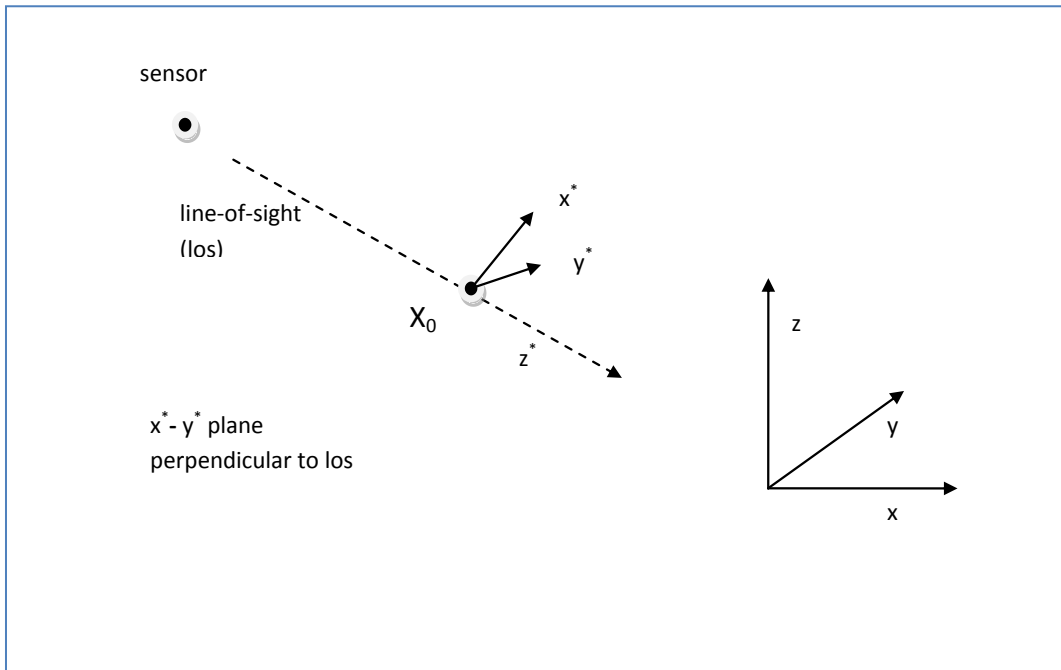


Figure I-1: RPC Uncertainty is represented in a plane perpendicular to the line-of-sight vector

The primary x-y-z ground coordinate system is assumed WGS-84 ECF, the coordinate system of the *i2g* output and *g2i* input via the CSM API. (When  $z_i$  is used as an input to an image-to-ground call, it is assumed (converted to) an elevation.)

The directions  $x^*$  and  $y^*$  are expressed in the primary coordinate system and are computed as follows, where  $los_i$  is the unit line-of-sight vector in the primary coordinate system and corresponds to grid point  $i$ :

$$los_i = \frac{i2g(l_i, s_i, z_i) - i2g(l_i, s_i, z_i + 100)}{\|i2g(l_i, s_i, z_i) - i2g(l_i, s_i, z_i + 100)\|} \quad (12)$$

Convert the above  $los_i$  to a local tangent plane representation:  $los_i \rightarrow \Phi_{PtoL} los_i$ , where  $\Phi_{PtoL}$  is the  $3 \times 3$  primary to local coordinate system (orthonormal) transformation matrix applicable at the ground (grid) point's nominal location  $X_{0i} = i2g(l_i, s_i, z_i)$ .

$$x_i^* = \frac{los_i \times [0 \ 0 \ 1]^T}{\|los_i \times [0 \ 0 \ 1]^T\|} \quad (13)$$

$$y_i^* = los_i \times x_i^* \quad (14)$$

The above calculations utilize the vector cross-product  $\times$ , and are based on the assumption that  $los_i \neq [0 \ 0 \ -1]^T$ , otherwise set  $x_i^* = [0 \ -1 \ 0]^T$  and  $y_i^* = [-1 \ 0 \ 0]^T$ .

Convert  $x_i^*$  and  $y_i^*$  from a local tangent plane representation to a primary coordinate system representation:  $x_i^* \rightarrow \Phi_{PtoL}^T x_i^*$  and  $y_i^* \rightarrow \Phi_{PtoL}^T y_i^*$ .

$$(15)$$

$$X_{0i} = i2g(l_i, s_i, z_i) \quad (16)$$

$$X_{1i} = X_{0i} + 20 x_i^* \quad (17)$$

$$X_{2i} = X_{0i} + 20 y_i^* \quad (18)$$

$$\begin{bmatrix} \frac{\partial l_i}{\partial x_i^*} & \frac{\partial s_i}{\partial x_i^*} \end{bmatrix}^T = \frac{g2i(X_{1i}) - g2i(X_{0i})}{20} \quad (19)$$

$$\begin{bmatrix} \frac{\partial l_i}{\partial y_i^*} & \frac{\partial s_i}{\partial y_i^*} \end{bmatrix}^T = \frac{g2i(X_{2i}) - g2i(X_{0i})}{20} \quad (110)$$

$$A_i = \begin{bmatrix} \frac{\partial l_i}{\partial x_i^*} & \frac{\partial l_i}{\partial y_i^*} \\ \frac{\partial s_i}{\partial x_i^*} & \frac{\partial s_i}{\partial y_i^*} \end{bmatrix} \quad (111)$$

The above  $A$  matrix is suitable for RPC uncertainty parameter generation and for mono error propagation. (The latter uses the *a priori* location for the ground point to be extracted instead of the grid point.) However, unlike for the baseline method, two different  $x^*$ - $y^*$  coordinate system definitions are required for stereo error propagation. The following details corresponding calculations.

### Stereo error propagation

The following describes the computation of the 2x2 matrix of partial derivatives of image coordinates with respect to ground plane coordinates. There are two such matrices, corresponding to a ground plane perpendicular to the image line-of-sight vector at the center of each image  $j = 1,2$ .

Specifically, there are two sets of ground plane coordinate systems:  $(x_1^*, y_1^*)$  and  $(x_2^*, y_2^*)$ , corresponding to  $A_1$  and  $A_2$ , respectively. The coordinate systems cannot be the same and also perpendicular to their corresponding unit line-of-sight vectors. Thus, define:

$$y_j^* \text{ in the direction of } (los_1 \times los_2), j = 1,2 \quad (I12)$$

$$x_j^* \text{ in the direction of } (los_1 \times los_2) \times los_j, j = 1,2. \quad (I13)$$

$$\text{Unitize the resultant } x_j^* \text{ and } y_j^*, j = 1,2. \quad (I14)$$

The computations I12-I14 are made with vectors represented in the primary coordinate system, including the line-of-sight vectors, for efficiency. Once computed, the  $x^*-y^*$  directions are then defined, and Equations I7-I11 then implemented in order to complete the derivation of  $A_j, j=1,2$ .

Note that the  $x^*$  directions are in the approximate stereo epipolar direction.

See Appendix J for further discussion on the selection of the  $(x_1^*, y_1^*)$  and  $(x_2^*, y_2^*)$  ground plane coordinate systems and their effect on error propagation. See Appendix K for the trade regarding use of the baseline horizontal ground plane versus use of a ground plane perpendicular to the line-of-sight vector in order to represent RPC uncertainty.

## Appendix J: Selection of x\*-y\* directions

This appendix addresses the effects that the selected x\*-y\* directions have on RPC uncertainty generation and error propagation. These directions are contained in the ground plane selected to represent RPC uncertainty.

The first part of the appendix (first two subsections) addresses the effects regarding generation of RPC uncertainty parameters and monoscopic error propagation. It will be shown that results are invariant to the particular ground plane selected, i.e., either the baseline horizontal tangent plane or alternatively a plane perpendicular to the imaging line-of-sight vector. It will also be shown that it doesn't matter which particular x\*-y\* directions are selected as long as they are perpendicular to each other and in the same ground plane.

The second part of the appendix addresses stereo error propagation. It will be shown that the specific directions chosen for x\*-y\* do affect results. It will also be shown that highest fidelity results correspond to the baseline method which uses the horizontal tangent plane for each image and common x\*-y\* directions (e.g., south and east, where south corresponds to approximate direction of flight and epipolar direction). If a ground plane perpendicular to the imaging line-of-sight vector (different for both images) is selected instead, the best x\*-y\* directions are presented which, by necessity, must differ between the two images in at least one-component.

### Generation of *er*, *eb*

For an arbitrary ground (grid) point, assume a new direction x'\*-y'\* in the ground plane (either the baseline horizontal tangent plane or alternatively a plane perpendicular to the line-of-sight vector) related to the original x\*-y\* directions by a 2x2 orthonormal transformation  $\Phi$ ; its corresponding  $A'^{-1} = \frac{\partial(x',y')}{\partial(l,s)} = \frac{\partial(x',y')}{\partial(x,y)} \frac{\partial(x,y)}{\partial(l,s)} = \Phi A^{-1}$ . Therefore (see Equation (1) in the main body of this document):

$$\begin{aligned} \sigma_s'^2 &= (CE\{A'^{-1}B_S P_S B_S^T A'^{-T}\}/2.15)^2 = (CE\{\Phi(A^{-1}B_S P_S B_S^T A^{-T})\Phi^T\}/2.15)^2 \\ &= (CE\{A^{-1}B_S P_S B_S^T A^{-T}\}/2.15)^2 = \sigma_s^2 \end{aligned}$$

The above is true since eigenvalues (not eigenvectors) are invariant under a similarity transformation (pre and post multiplication by  $\Phi$  and  $\Phi^T$ , respectively). (See Meyer, C.D., Matrix Analysis and Applied Linear Algebra, pg 508, SIAM, 2008.) This also implies that  $CE\{\}$  is invariant since it is solely a function of the eigenvalues of the covariance matrix.

Thus, the calculation of  $\sigma_s$  (as well as  $\sigma_{TU}$  by similar analysis) is invariant of the selected x\*-y\* directions; correspondingly, the generation of *er*, and *eb* is also invariant.

### Monoscopic absolute and relative error propagation

Because  $A'^{-1} = \Phi A^{-1}$ , this implies that  $A' = A\Phi^{-1} = A\Phi^T$  and  $A = A'\Phi$ . Therefore, the key component of monoscopic error propagation (see Equations (17) and (26) in the main body of this document) is equal to:

$$P_{OR} = eb^2 A' A'^T = eb^2 A \Phi^T \Phi A^T = eb^2 A A^T,$$

i.e., invariant (a similar analysis is also applicable to  $P_{TUi}$ ).

Thus, monoscopic absolute and relative error propagation are invariant to the particular  $x^*$ - $y^*$  directions chosen by the error propagation function for the image.

### Stereo (absolute) error propagation

However, for stereo error propagation when there is non-zero temporal correlation between the two images, results are not invariant to the selection of the  $x^*$ - $y^*$  directions for the two images.

Let us examine the key intermediate stereo error propagation quantity presented below, where  $A_j$  corresponds to the center of image  $j = 1,2$ , and was computed based on the ground plane selected to represent RPC uncertainty and the directions  $x^*$  and  $y^*$  contained in the plane. In general, the  $x^*$  and  $y^*$  directions can differ between images.

This intermediate error propagation quantity is the  $4 \times 4$  error covariance matrix relative to image space and corresponding to the *a priori* uncertainty in the RPC adjustable parameters (see Equations (35), (38), and (40) in the main body of this document):

$$\begin{bmatrix} P_{OR11} & P_{OR12} \\ P_{OR12}^T & P_{OR22} \end{bmatrix} = \begin{bmatrix} (eb_1^2)A_1A_1^T & (\rho eb_1 eb_2)A_1A_2^T \\ (\rho eb_1 eb_2)A_2A_1^T & (eb_2^2)A_2A_2^T \end{bmatrix}.$$

By similar analysis as for monoscopic error propagation, the (scaled) diagonal blocks  $A_j A_j^T$  are invariant to the particular  $x^*$ - $y^*$  system chosen. However, there can be a “problem” associated with the cross-block or cross-covariance between the two images.

Let us reformulate the above as:

$$\begin{bmatrix} P_{OR11} & P_{OR12} \\ P_{OR12}^T & P_{OR22} \end{bmatrix} = \begin{bmatrix} (eb_1^2)A_1A_1^T & (\rho eb_1 eb_2)A_1A_2^T \\ (\rho eb_1 eb_2)A_2A_1^T & (eb_2^2)A_2A_2^T \end{bmatrix} = \begin{bmatrix} A_1 & 0 \\ 0 & A_2 \end{bmatrix} \begin{bmatrix} (eb_1^2)I_{2 \times 2} & (\rho eb_1 eb_2)I_{2 \times 2} \\ (\rho eb_1 eb_2)I_{2 \times 2} & (eb_2^2)I_{2 \times 2} \end{bmatrix} \begin{bmatrix} A_1^T & 0 \\ 0 & A_2^T \end{bmatrix}.$$

The interior matrix corresponds to the  $4 \times 4$  error covariance of RPC sensor support data errors for the two images relative to the  $x^*-y^*$  ground plane coordinate systems. These are “organic” RPC support data errors as represented in the ground planes for the two images.

The cross term  $(\rho eb_1 eb_2)I_{2 \times 2}$  corresponds to the correlation of errors between the components of the two  $2 \times 1$  organic RPC support data error vectors. It is desirable that this same correlation is also applicable for an arbitrary but common geographic direction. That is, we make the reasonable assumption that the effect of positive temporal correlation of support data errors should have the same geographically-aligned effect for both same-pass images. In other words, whatever the effect of support data error for image 1 in a specific yet arbitrary direction in a geographically aligned 3D coordinate system, the (correlated) support data error for image 2 should have the same effect in that direction. However, this only occurs if the two  $x^*-y^*$  systems are the same, i.e., aligned, as demonstrated below:

Let the  $3 \times 3$  matrix  $\Gamma_j$  represent the transformation from the  $x^*-y^*-z^*$  system corresponding to image  $j$  to a (common) 3D geographic system, such as a local tangent plane coordinate system. Let  $r_j = [r_{x^*j} \ r_{y^*j} \ 0]^T$  represent the  $3 \times 1$  vector of RPC errors in the  $x^*-y^*-z^*$  system. (The uncertainty in the  $z^*$  direction does not correspond to an RPC error.) Let  $r'_j = \Gamma_j r_j$  represent this same error but as represented in the geographic system. Let  $u^T r'_j$  represent the (unit) projection of this error along an arbitrary direction  $u$  in the geographic system. The (scalar) cross-covariance of the projected errors corresponding to the two images equals:

$$E\{u^T r'_1 (u^T r'_2)^T\} = u^T E\{r'_1 r'^T_2\}u = u^T \Gamma_1 E\{r_1 r^T_2\} \Gamma^T_2 u = u^T \Gamma_1 \begin{bmatrix} \rho eb_1 eb_2 I_{2 \times 2} & 0 \\ 0 & 0 \end{bmatrix} \Gamma^T_2 u = \rho eb_1 eb_2 u^T \Gamma_1 \begin{bmatrix} I_{2 \times 2} & 0 \\ 0 & 0 \end{bmatrix} \Gamma^T_2 u .$$

The (scalar) variance for image  $j$  equals:

$$E\{u^T r'_j (u^T r'_j)^T\} = u^T E\{r'_j r'^T_j\}u = u^T \Gamma_j E\{r_j r^T_j\} \Gamma^T_j u = eb_j^2 u^T \Gamma_j \begin{bmatrix} I_{2 \times 2} & 0 \\ 0 & 0 \end{bmatrix} \Gamma^T_j u .$$

Therefore, the correlation coefficient equals:

$$\frac{\rho eb_1 eb_2 u^T \Gamma_1 \begin{bmatrix} I_{2 \times 2} & 0 \\ 0 & 0 \end{bmatrix} \Gamma^T_2 u}{\left( (eb_1^2 u^T \Gamma_1 \begin{bmatrix} I_{2 \times 2} & 0 \\ 0 & 0 \end{bmatrix} \Gamma^T_1 u) (eb_2^2 u^T \Gamma_2 \begin{bmatrix} I_{2 \times 2} & 0 \\ 0 & 0 \end{bmatrix} \Gamma^T_2 u) \right)^{1/2}} , \text{ which equals } \rho \text{ for an arbitrary direction } u \text{ if and}$$

only if  $\Gamma_1 = \Gamma_2$ , which implies that the  $x^*-y^*-z^*$  (hence,  $x^*-y^*$ ) must be aligned for the two images.

(Note that the variance for image  $j$  is greater than or equal to 0 since  $\begin{bmatrix} I_{2 \times 2} & 0 \\ 0 & 0 \end{bmatrix}$  is a rank 2 positive semi-definite matrix,  $\Gamma_j \begin{bmatrix} I_{2 \times 2} & 0 \\ 0 & 0 \end{bmatrix} \Gamma^T_j$  is also a rank 2 positive semi-definite matrix since

$\Gamma_j$  is full rank 3, and hence by the definition of positive semi-definite,  $u^T \Gamma_j \begin{bmatrix} I_{2 \times 2} & 0 \\ 0 & 0 \end{bmatrix} \Gamma_j^T u \geq 0$  for all non-zero vectors  $u$ ; correspondingly, there will also be a direction  $u$  for which there is zero uncertainty and hence,  $\rho$  undefined for that particular direction.)

We obtain the desired property that  $x^*-y^*$  are aligned for the two images if the ground plane for each image is the local horizontal tangent plane corresponding to the center of the image and that the  $x^*-y^*$  directions are common in the two ground planes, i.e., south and east. (The directions of  $x^*-y^*$  in the two planes when expressed in the primary coordinate system are not exactly the same but are very close since the image footprints overlap.)

However, this is not the case if the ground planes selected for the two images are perpendicular to each image's line-of-sight vector. For this case, we make a realistic compromise that achieves approximately the same geographic support data error correlation for both same-pass images while maintaining perpendicularity to each image los. Specifically, we define the  $x^*-y^*$  systems for the two images in a similar and geographic manner as follows:

$y_j^*$  in the direction of  $(los_1 \times los_2)$ ,  $j = 1,2$

$x_j^*$  in the direction of  $(los_1 \times los_2) \times los_j$ ,  $j = 1,2$ , where the  $x_j^*$  directions correspond to the approximate stereo "base".

The two  $x^*-y^*$  systems are closely, but not perfectly, aligned. The above algorithm is that reflected in Appendix I.

(Note: all of the above stereo correlation analysis is unaffected by the direction of the image coordinate axes relative to geographic space. Any effects are automatically handled via the  $A_j$  matrices.)

(Note: we expect the following dominant sensor support data errors to be geographically positively correlated for a same-pass pair of images:

- (1) sensor position errors
- (2) all sensor attitude errors (star tracker related and scanning related) if both images are scanned in the same direction (forward/forward or reverse/reverse)
- (3) star tracker related attitude errors regardless scan directions.

Thus, in general and given no other ancillary information, we expect that the effect of total support data errors to be geographically positively correlated for a stereo pair of images.)

(Note: for multi-image extraction/error propagation involving more than two same-pass images, there is no further complication if the baseline method is used. However, if a ground plane perpendicular to the line-of-sight vector is used, compute the  $x^*-y^*$  directions (and  $A$  matrices)

as described above for each pair in imaging order. And for an image with two sets of  $x^*-y^*$  directions (and  $A$  matrices), take their average.)

## Appendix K: Trade Studies

Two trade studies were performed and are documented in this appendix. One was relatively simple and intuitive and concerned the definition of the RPC adjustable parameters. Image-space adjustable parameters were selected. In particular, line and sample offset parameters, with RPC uncertainty as represented by  $er$  and  $eb$  mapped to adjustable parameter *a priori* uncertainty at the center of the image using the corresponding  $A$  matrix.

The second trade study was more challenging – the selection of the ground plane used to represent RPC uncertainty. Its resolution involved both “operational” issues regarding the generation and application of RPC uncertainty parameters as well as metric performance comparisons between the two candidates. The two candidates were: (1) the local horizontal tangent plane, and (2) a ground plane perpendicular to the imaging line-of-sight. The former was selected for reasons detailed throughout this appendix and summarized at its end.

The second trade study also explored some of the inherent characteristics and limitations of RPC, independent of the ground plane used to represent RPC uncertainty.

THE REMAINDER OF THIS APPENDIX WAS REMOVED IN THIS VERSION OF THE DOCUMENT AS CONSIDERED: *company sensitive*.